

1 *Responses to*

2 *Interactive comment on “Abrupt seasonal transitions in land carbon uptake in*
3 *2015” by Chao Yue et al.*

4 **Anonymous Referee #1**

5 Received and published: 19 February 2017

6 The article “Abrupt seasonal transitions in land carbon uptake in 2015” by C. Yue and coauthors presents
7 a detailed analysis of anomalies in carbon sinks and sources, climate and vegetation greenness during
8 recent decades with an emphasis on the year 2015. Understanding the carbon cycle and its interaction
9 with climate change is a highly relevant research topic, and the authors refer to state-of-the-art literature
10 and datasets. The authors combine a number of observational datasets and model results, and my
11 impression is that their methods and results are sound. The description of the work steps is clear and the
12 data sources are well documented. In this regard, the article is good at what it does.

13 My major concern however is that it remains unclear what the authors are trying to achieve with this
14 article. I would guess that the results might tell us something about how climate affects vegetation and the
15 carbon cycle. What do the results imply about the relevant processes, about past climates and potential
16 future developments, or about our potential to model these processes? The authors address such questions
17 only briefly in the last paragraph of Sect. 4 and in the very short Sect. 5, stating that they go beyond the
18 scope of the article.

19 [Response] We thank the general positive comments by the reviewer. We were originally aiming for two
20 purposes in this article: (a) to diagnose the anomaly of large scale CO₂ fluxes for 2015 given the specific
21 nature of that year, as a case study (high CO₂ growth rate, anomalously strong vegetation greenness and
22 the historically highest annual temperature), using atmospheric inversion data, and (b) to diagnose
23 whether abrupt transitions have occurred in terrestrial carbon uptake in 2015, and briefly infer the reasons
24 for such transitions.

25 We agree with reviewer that the exploration of the general links among vegetation greenness, land carbon
26 uptake dynamics and climate variations is necessary in order to put the 2015 case into a more general
27 picture, to infer general patterns of land carbon dynamics that could be useful for future prediction of land
28 carbon dynamics. We add this point as one of the research aims of our paper. According changes are

29 made in revised abstract, and the 3rd paragraph of the revised Introduction section.

30 We have extensively revised the manuscript to incorporate correlations of land carbon uptake anomalies
31 with vegetation greenness anomalies and climate anomalies related with ENSO dynamics. Two new
32 figures (Fig. 3, Fig. 4) are added in the main text, and three new figures (Fig. S4, S5, S7) are added in the
33 Supplementary Material. Results and discussion sections are substantially expanded to include more
34 discussions on the mechanisms underlying land carbon dynamics relevant to the purpose of this study.

35 I also wonder why the authors focus so much on the year 2015. What is so special about this year (apart
36 from being relatively recent) that would justify this focus, and what can we learn from this case study that
37 is valid in a greater context? If there is something I am overlooking, I suggest that the authors reframe
38 their article to bring out their message more explicitly, and that they stress what the progress is compared
39 to previous articles. I believe that this would improve the impact of their article. For example, the authors
40 could systematically relate anomalies in climate, carbon fluxes and NDVI using the whole record, and not
41 only focus on 2015. They should also consider to include the year 2016 (if possible) to capture the full
42 recent El Nino event. It appears a bit arbitrary that they pick the year 2015 and one other previous El Nino
43 event for their analysis, using the rest of their data only to calculate linear trends. A more comprehensive
44 statistical analysis of the available data might allow more general conclusions without the need of running
45 climate models.

46 So far, the main selling points of the paper seem to be

47 (i) the (arguably) counterintuitive combination of high NDVI and negative carbon uptake anomaly (ii)
48 large anomaly of the year 2015.

49 Regarding (i), I find it little surprising that greening and carbon loss (or a reduced carbon sink) can go
50 together since both anomalies can be dominated by different locations and different seasons, and because
51 they are not linearly related given the complex ecological processes involved. The authors point this out
52 themselves, hence invoking a “paradox” seems a little exaggerated to my taste. (But I would be curious if
53 this anti- correlation is a temporal feature or a robust trend that can be expected to continue in the future;
54 something the authors might choose to give more attention to.) Regarding (ii), I find it misleading to
55 speak of an “abrupt transition” (title, abstract and line 263+). This term gives the impression of a singular
56 event with long-lasting consequences, like a forced non-reversible switch to another state or regime.
57 However, the phenomenon discussed in the paper appears to be an anomaly that is the realisation of
58 natural variability, hence an extreme but temporal event. This comes on top of a gradual trend to larger
59 growth rates, so the year 2015 will most likely not be unique. In fact, the atmospheric growth rate of CO₂

60 in 2016 was even higher than in 2015. I therefore wonder whether the term “abrupt transition” is useful
61 here, and would suggest a more suitable term, e.g. the land carbon uptake anomaly in 2015. I therefore
62 also strongly suggest a change in the paper’s title.

63 [Response]

64 (1) We now use the full 1981–2015 data and performed statistical analysis of vegetation greenness, land
65 carbon uptake and climate anomalies for different regions and seasons. These results are incorporated in
66 the revised manuscript in both result and discussion sections, with findings from previous studies being
67 extensively referred to and discussed as well.

68 (2) We maintain the “paradox” expression because we think it is adequate to describe the year 2015,
69 which comes with extreme greenness and an only moderate land carbon sink. Higher greenness is
70 sometimes simply assumed to be associated with higher sink, but this is not necessarily true, as is also
71 pointed out by the reviewer. We now examine in more detail in the revised the relationship between land
72 carbon uptake and vegetation greenness for different seasons and regions.

73 (3) As explained in the response to the previous comment, now the manuscript is restructured around two
74 research aims: to examine general relationships among vegetation greenness, land carbon uptake and
75 climate variations, and to examine the 2015 as a special case on how land carbon dynamics have
76 responded to a combination of extreme greenness and ENSO climate variations. This is made clear in the
77 revised manuscript. According changes are made in the title of the paper, abstract, 3rd paragraph of the
78 “Introduction” section, results and discussion.

79 (4) We mostly drop the word ‘abrupt’ given its potential confusion in an ecological context and, instead,
80 the word “strong” is used.

81 (5) We change the title to reflect the revision in the manuscript content to “Vegetation greenness and land
82 carbon flux anomaly associated with climate variations with a special focus on the year 2015”.

83 (6) We did not include the year 2016 into the current analysis because the inversion data are not available
84 yet. But we believe focusing on the year 2015 could already generate meaningful conclusions from our
85 manuscript.

86 Minor comments

87 - line 85-86: “We used ... includes”

88 [Response] we changed ‘includes’ to ‘including’.

89 - line 89: What is a validity period, and in what sense are the other years are not valid?

90 [Response] Site observations used in the Jena CarboScope inversion are coherent over time within the so-
91 called “validity period”, but are not outside the validity period. More specifically, the validity period is
92 defined by the one using a consistent number of sites, i.e., all sites that have observations over such a
93 period. Outside the validity period, site numbers changed depending on their availability or operation
94 time. It is optimal to examine the temporal trend within the validity period, but this does not mean the
95 data outside this period are invalid and should not be used. In fact, the same situation also happens for the
96 CAMS inversion, which considers a variable number of sites during the full study period. Because our
97 analysis has to reconcile the need of a large site number in 2015 and long historical period for a robust
98 anomaly estimate, using the s04_v3.8 run outside its validity period is therefore a compromise. Besides
99 the responses here, we made the according changes in Section 2.1.1.

100 - line 108: Why do the authors pick MAI to characterise the ENSO state?

101 [Response] We believe the reviewer means MEI rather than MAI. MEI (Multivariate ENSO Index) is the
102 first unrotated principal component of six variables over the tropical Pacific that are closely linked with
103 ENSO. Among the six variables sea-level pressure, sea surface temperature and surface air temperature
104 are included. MEI has been widely used in literature as an indicator for the ENSO state, for instance,
105 Nemani et al., 2003; Wang et al., 2013; van der Werf et al., 2008. The MEI should, therefore, summarize
106 not only the ocean component of ENSO (El-Niño), but also the atmospheric component (the Southern
107 Oscillation).

108 As a complement to MEI, we also used the Oceanic Niño Index (ONI,
109 http://www.cpc.ncep.noaa.gov/products/analysis_monitoring/ensostuff/ONI_change.shtml) when
110 comparing the evolution of El Niño events of 1997 and 2015 in Supplementary Figure S10. The ONI
111 tracks the running 3-month average sea surface temperatures in the east-central tropical Pacific between
112 120°-170°W (the Niño 3.4 region). Supplementary Figure S10 shows very similar temporal patterns of
113 MEI and ONI during El Niño evolution especially when El Niño reached its peak, indicating the
114 suitability of MEI being used in ENSO-related analysis.

115 The pieces of information described above are also included in the revised manuscript in appropriate
116 sections (section 2.1.3, 1st paragraph of section 4.2).

117 - line 141-148. At the first reading I did not understand the role of the “historical trend” for the growth

118 rate in a given year. I understand now that specific anomalies in 2015 are later related to climate
119 anomalies, with anomalies being defined as residuals after removing a linear trend. The reasoning behind
120 this could be explained more explicitly here.

121 [Response] We added the following text in this paragraph (1st paragraph of section 2.2.2) to make it more
122 explicit and hope it will help clarify better: “The record-breaking AGR in 2015 thus must be put into an
123 historical perspective to reconcile evidence for extreme greening and the highest atmospheric CO₂
124 growth rate. For example, if 2015 comes up with a large increase in carbon emissions accompanied by
125 droughts (browning) in the northern hemisphere and the tropics, then the highest AGR might not be
126 regarded as a big surprise. Therefore, to understand the contributing factors for the highest AGR in 2015,
127 it must be separated into a long-term trend and interannual anomalies.”

128 - line 201: both instead of bother

129 [Response] This has been corrected.

130 - line 136: It would help non-experts to briefly explain how the sources and sinks are quantified in the
131 GCP. How independent is this dataset from the inversion calculations?

132 [Response] Estimates of land and ocean carbon uptakes are largely independent from the two inversions
133 used in this study. We have inserted the following text in this paragraph (last paragraph of section 2.1.1)
134 to clarify this: “Estimates of ocean carbon uptake in GCP are based on observation-based mean CO₂ sink
135 estimate for the 1990s and variability in the ocean CO₂ sink for 1959–2015 from global ocean
136 biogeochemistry models. Estimates of land carbon uptake in GCP are calculated as the difference
137 between anthropogenic emissions, atmospheric CO₂ growth and ocean sink. The estimates of land and
138 ocean carbon uptake in GCP are largely independent from the two inversions used here, except that the
139 CO₂ records from atmospheric stations which are used in inversions are also used in GCP to derive global
140 AGR.”

141 - Sect. 2.2.1: It would help me to already see time series and a map as a visualisation of the rank analysis.
142 I understand the structure of the paper and find it reasonable, but it could make sense to merge the data
143 analysis section 2.2 with Results Sect. 3. Otherwise, one has to read the methods section without
144 visualisation, and later remember each methodological detail when the results are shown. This is a matter
145 of taste and I leave it to the authors to reconsider the structure.

146 [Response] Relevant figures (Fig. 1, Supplementary Fig. S1, Supplementary Fig. S3) are now cited in this
147 section in the revised manuscript to help readers understand better the methods. But we maintained the

- 148 [methods and result as two separate sections mainly for the clarity of the structure.](#)
- 149 - line 226: “the seemingly paradox” is grammatically wrong.
- 150 [\[Response\] “seemingly” is changed to “seeming”.](#)
- 151 - line 350: data suggests (not suggest)
- 152 [\[Response\] Corrected.](#)
- 153 - Supplementary Material: I suggest to put captions underneath (not above) the figures and increase the
154 space between the figures. There is too much space between the caption of Fig. 2 and Fig. 2. These things
155 make it difficult to identify the right caption for each figure.
- 156 [\[Response\] Figure captions are now put below figures.](#)

157 *Responses to*

158 *Review comments of “Abrupt seasonal transitions in land carbon uptake in*
159 *2015” by Chao Yue et al.*

160 **Matthias Forkel, 2017-03-08**

161 **1. Does the paper address relevant scientific questions within the scope of ACP?**

162 The article by C. Yue et al. addresses annual and seasonal variabilities in global land carbon uptake and
163 the relations with climate and vegetation. This paper is within the scope of ACP.

164 **2. Does the paper present novel concepts, ideas, tools, or data?**

165 The paper is based on well established datasets and methods to generate such data (CO₂ measurements,
166 NDVI data, atmospheric inversion). The title and the abstract of the paper mainly highlights one finding
167 of the study about "abrupt seasonal transitions in land carbon uptake". This finding is not really new
168 (except the focus on 2015) but the results of the study are a good opportunity to remind the land carbon
169 cycle community about such mechanisms and to point to the year 2015 as a remarkable example of such
170 seasonal transitions.

171 **3. Are substantial conclusions reached?**

172 The entire study is focussed on anomalies of the land carbon uptake in the year 2015 relative to the period
173 1981 to 2015. Consequently, the conclusions are very specific for climate/carbon cycle mechanism in this
174 year. To make this paper more interesting for the land carbon cycle community and to reach more
175 substantial and less specific conclusions, I would recommend to perform similar analyses also for other
176 years and to finally draw conclusions about general mechanisms in comparison to specificities in single
177 years. In this point, I completely agree with Anonymous Referee #1.

178 [Response] We examined extensively the relationship between anomalies in land carbon uptake, NDVI
179 and climate variations. These new analyses are incorporated in the substantially revised results and
180 discussion section.

181 **4. Are the scientific methods and assumptions valid and clearly outlined?**

182 Overall, yes. For some datasets, I would expect scientific references additionally to the URLs from which

183 the data was obtained (especially in Sections 2.2.2 and 2.2.3). The only exception is the analysis of NDVI
184 data (Section 2.2.1): For example, the authors calculated “seasonal mean standardized NDVI”. Although I
185 have some experience with NDVI data (Forkel et al., 2013), I cannot imagine what this term means. How
186 were NDVI values standardized? Why? Furthermore, mean NDVI values of winter seasons in northern
187 regions are not very useful to draw conclusions about vegetation productivity or land carbon uptake. As
188 NDVI is a land surface property it is not only affected by vegetation but outside the peak of the growing
189 season strongly by changes in snow cover and soil reflectance. Consequently, a certain ranking in a
190 season especially in northern regions might be due to the variability in snow cover but not in vegetation.
191 The authors need to appropriate filter the NDVI time series to separate vegetation signals from other non-
192 vegetation distortions (Hird and McDermid, 2009; Holben, 1986; Kandasamy et al., 2013). Furthermore,
193 NDVI datasets from different sensors show large differences which are especially important for seasonal
194 anomalies that are outside of the peak of the growing season (D’Odorico et al., 2014; Fensholt and Proud,
195 2012; Kern et al., 2016; Scheftic et al., 2014). Consequently, I’m wondering if the shown ranking of
196 seasonal NDVI values (Fig. 1) is a robust result given the noise of NDVI data and the differences between
197 datasets. This rises the question if 2015 is indeed the greenest year.

198 [Response] The scientific citations for MEI and NDVI are provided in additional to URL links. NDVI
199 reflects in general vegetation green fraction, and is considered as a proxy of green leaf area (Gamon et al.,
200 1995; Ide et al., 2010) Its temporal magnitudes have been used to infer changes in vegetation productivity
201 (Myneni et al., 1997; Zhao and Running, 2010). In response to the reviewer’s comments, we have
202 updated our results by using a new NDVI data set that went through rigorous quality control, with the
203 cloud- and snow-contaminated pixels being removed and gap-filled. Note that the original NDVI values,
204 rather than standardized anomalies, are used. Seasonal NDVI values lower than 0.1 were further removed
205 to make sure the used NDVI values reflect the dominance of vegetation information.

206
207 Because of filtering NDVI values by a minimum of 0.1, we are cautiously confident that the vegetation
208 greenness reflects (at least partly) the vegetation information even in the first (Q1) and fourth (Q4)
209 trimester of the year when snow is present in the northern hemisphere. In fact, October is frequently
210 considered within the growing season and some evergreen coniferous forests show significant
211 photosynthetic activities in March in regions of mild winter, e.g., Tanja et al., 2003). Here we show that,
212 most of the grid cells where 2015 shows the highest NDVI for northern land (Fig. CS1, region with
213 latitude > 30°N) are in fact dominated by Q2 (April–June) and Q3 (July–September), corresponding
214 roughly to northern hemisphere growing season. The vegetated land area (i.e., with a seasonal NDVI
215 value higher than 0.1 in either of the four seasons of 2015) with the highest NDVI rank in 2015 in the

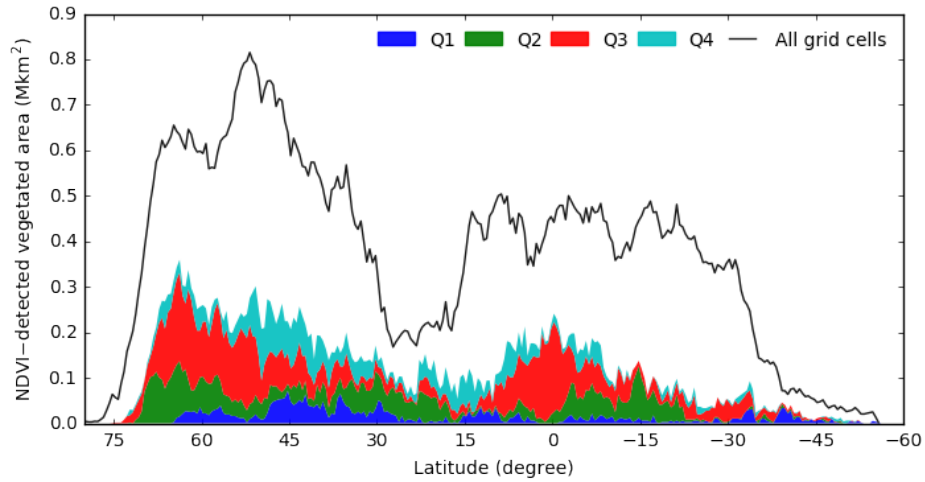
216 northern land accounts for 36% of all land area, in contrast with an expected mean of 6.25% if the land is
217 equally green over all years of 2000–2015. This highlights again the extreme greening during the growing
218 season in the northern hemisphere in 2015, as has been examined in more detail in Bastos et al. (2017).

219
220 Q1 and Q4 account for 34% of the land area where 2015 NDVI ranks the highest in northern land. These
221 grid cells are either dominated by evergreen forests (central Canada, northwestern Europe), or by oceanic
222 climate where evergreen forests prevail (eastern Canada and US, Europe) (Fig. CS2). As shown in Fig.
223 CS3, the land north to 23.5°N contributes primarily to the overall highest annual NDVI in 2015, whereas
224 in tropics (23.5°S–23.5°N) and southern extra-tropics (latitude > 23.5°S), the NDVI in 2015 is only
225 moderately high (0–23.5°N) or around the multi-annual mean value (southern hemisphere).

226
227 Therefore, we conclude that, globally, 2015 is the greenest year of 2000–2015, in terms of both the mean
228 annual NDVI value, and the number of grid cells where NDVI shows the highest rank in 2000–2015. This
229 greenest signal is dominated by the extreme greenness in the growing season of the northern hemisphere,
230 which has been examined in details in Bastos et al. (2017) and identified as a robust phenomenon
231 independent of different satellite sensors used, or quality control procedures of the data. The Fig. S1 in
232 Bastos et al. (2017) confirmed that both data from Terra and Aqua sensors show that 2015 has the highest
233 growing season NDVI in 2000–2015. They also confirmed that such a conclusion is consistent among
234 three quality control strategies of the Terra MODIS data used (Page 3, Bastos et al. 2017).

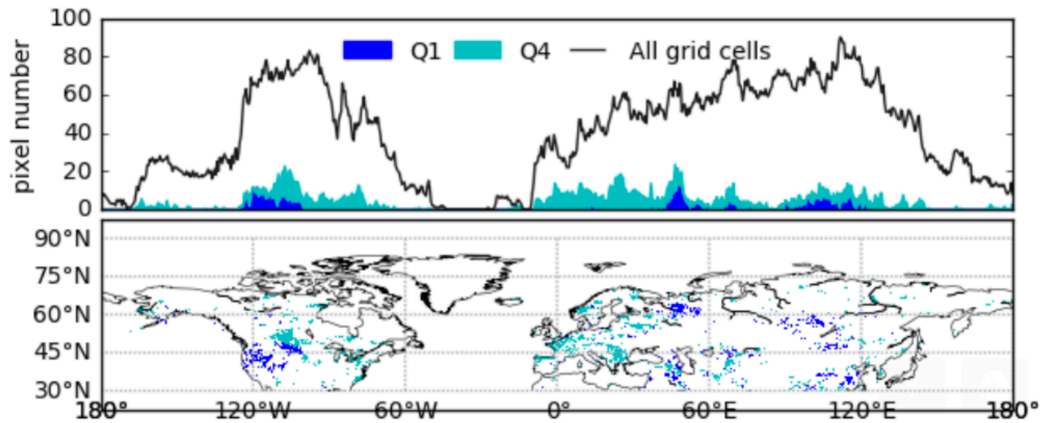
235
236 As the extreme greenness in 2015 is used as a starting point for our study and the main objective of our
237 paper is to report the carbon dynamics and seasonal shifts in land carbon uptake associated with climate
238 variations. We're fairly confident that sufficient evidences have been provided regarding the vegetation
239 greenness for this specific year.

240
241 Relevant revisions are made in the main text and the Supplement (section 2.1.2, section 2.2.1, and 2nd
242 paragraph of section 3.1 in the main text, and Supplement Fig. S2, Fig. S3).



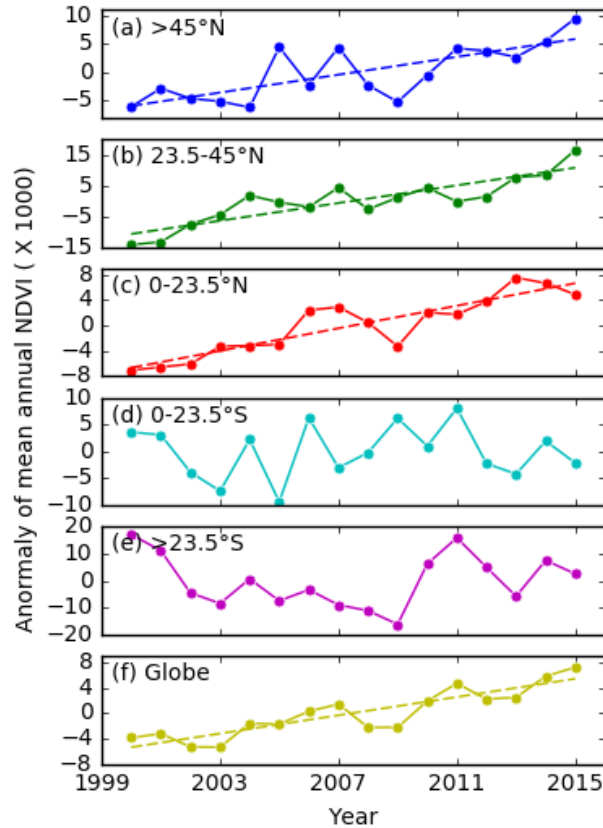
243
244
245

Fig. CS1 Seasonal distributions of land areas where 2015 shows the highest NDVI since 2000 as a function of latitude. Shaded areas represent different seasons stacked on top of each other.



246
247
248
249
250

Fig. CS2 (Top) Longitudinal distribution of the number of grid cells where 2015 NDVI ranks the highest in Q1 or Q4 of 2015 for the northern lands (latitude > 30°N). (Bottom) Spatial distribution of grid cells where NDVIs rank the highest for 2015 in Q1 or Q4 for the northern land (latitude > 30°N).



251

252 Fig. CS3 Annual NDVI anomalies for different latitudinal bands. The trend line is shown only for regions
 253 where significant simple linear regression over time is obtained.

254

255 **5. Are the results sufficient to support the interpretations and conclusions?**

256 Apart from the NDVI issues described above, the results are described in great detail and support the
 257 interpretation and conclusions.

258 [Response] Please refer to the responses to the comment above regarding the NDVI.

259 **6. Is the description of experiments and calculations sufficiently complete and precise to allow their
 260 reproduction by fellow scientists (traceability of results)?**

261 The calculations are mostly well described. The calculation of seasonal NDVI ranks seems to be a new
 262 approach to analyse NDVI time series (at least no reference is provided). Therefore I would recommend
 263 that the authors present some more details on this approach (at least in the Supplement) and ideally could
 264 provide also the code.

265 [Response] The NDVI ranking is mainly used to show the spatial distribution of abnormal greening in

266 2015, and that 2015 is in general the greenest year over 2000-2015 across the globe, which is dominated
267 by extreme greening in northern land. Please also refer to our responses to the Comment 4 for more
268 information. Fig. S3 in the revised Supplement shows the NDVI anomalies for different latitude bands,
269 which clearly indicate that the highest annual NDVI over the globe is driven by the extreme green
270 anomaly in the northern land ($>23.5^{\circ}\text{N}$). The code used to generate Figure 1 in the texts is made available
271 through a public repository (<https://github.com/ChaoYue/ACPD-2016-1167>).

272 **7. Do the authors give proper credit to related work and clearly indicate their own new/original**
273 **contribution?**

274 Yes. The cited literature is relevant for this study. The own contributions of the authors are clear.
275 However, I would recommend to provide a more detailed discussion on the link between vegetation
276 greenness from satellites and carbon cycle or atmospheric CO_2 variability in order to improve the
277 discussion section that is currently strongly focussed on the specificities of the year 2015. The results of
278 this paper could be for example discussed with respect to the following relevant papers (Angert et al.,
279 2005; Forkel et al., 2016; Gonsamo et al., 2017; Keenan et al., 2016; Myneni et al., 1997; Thomas et al.,
280 2016).

281 [Response] We have substantially strengthened the discussion by making new analysis regarding the links
282 among vegetation greenness, land carbon uptake anomalies and climate variations (Fig. 3, Fig. 4 in
283 revised manuscript, Fig. S4, S5, S7 in the revised Supplement). Please also refer to our responses to the
284 #2 Response to the comments by #1 reviewer.

285 **8. Does the title clearly reflect the contents of the paper?**

286 Yes. However, I recommend to extent the analysis to more years to draw less specific conclusions for a
287 single years. This might imply to change the title accordingly.

288 [Response] We extended the analysis by including more years and provided new figures in both main
289 texts and the Supplement. Please also refer to our responses to the first and second comment by #1
290 reviewer. The manuscript title is also changed to: Vegetation greenness and land carbon flux anomaly
291 associated with climate variations with a special focus on the year 2015.

292 **9. Does the abstract provide a concise and complete summary?**

293 Yes. The abstract is well written.

294 [Response] The abstract is updated to reflect the additional analysis that is conducted.

295 **10. Is the overall presentation well structured and clear?**

296 Yes.

297 **11. Is the language fluent and precise?**

298 Yes (as far as I can judge this). Some sentences are however too long and thus difficult to read, for
299 example: lines 74-78, 90-93,

300 [Response] These sentences are re-phrased to enhance their readability.

301 **12. Are mathematical formulae, symbols, abbreviations, and units correctly defined and used?**

302 Yes. Units and proper axis descriptions are missing in Fig. 4.

303 [Response] This is fixed.

304 **13. Should any parts of the paper (text, formulae, figures, tables) be clarified, reduced, combined,
305 or eliminated?**

306 Lines 71-74 are repeating lines 58-61 and can be merged.

307 [Response] Lines 58–61 are removed as they’re repeated in section 2.1.1.

308 Lines 81-93: The affect of station network density on the inversion is well described for the CarboScope
309 product. According to my understanding, the CAMS inversion should have the same problems. Please
310 clarify how these issued are handled in the CAMS inversion.

311 [Response] The CAMS inversion uses sites with at least 5-year worth of data. It therefore has a denser
312 (during the recent decade) but temporally evolving data coverage than Carboscope. The evolving network
313 in CAMS causes changes in inverted CO₂ fluxes that are superimposed on changes from biogeochemical
314 drivers during the whole period. Relevant revised texts are inserted in lines 116–119, on Page 4.

315 Lines 131-139: Please make clear why the conversion from ppm to PgC was done and if there is any
316 relevant uncertainty in this conversion factor.

317 [Response] The conversion of ppm to PgC is to express the atmospheric ‘sink’ of CO₂ in the same unit as

318 carbon fluxes diagnosed from inversions, in order to coherently assess contributions from different fluxes
319 to the AGR in 2015. This is explained in the revised texts. We used a conversion factor of $1 \text{ ppm CO}_2 =$
320 2.12 Pg C (Ciais et al., 2014; Prather et al., 2012). For multi-decadal analysis, this ratio is correct given
321 the sufficient mixing of CO_2 in the atmosphere because the value of $2.12 \text{ Pg C ppm}^{-1}$ considers the effect
322 of a flux equilibrated with the troposphere (mixed in ≈ 1.2 years) and the stratosphere (mixed in ≈ 5
323 years). However we used this ratio on an annual basis, with the assumption that the entire atmosphere is
324 well mixed within one year. This approximation is explicitly stated in the main text.

325 Such a ratio is mainly based on Ballantyne et al. (2012) & Le Quéré et al. (2016). We admit there are
326 uncertainties in this ratio. Ballantyne et al. (2012) gave a relatively detailed discussion in their methods.
327 On the one hand, the stratosphere is less well mixed with CO_2 than the troposphere, using CO_2
328 measurements at marine boundary layer (MBL) might overestimated the atmospheric CO_2 sink (thus
329 implying a ratio that should be smaller than 2.12). But on the other hand, there is also CO_2 gradient from
330 the continental boundary layer to marine boundary layer, which could compensate for the insufficient
331 mixing in the stratosphere. Ballantyne et al. (2012) finally reached the conclusion that these two factors
332 roughly cancel out each other by citing the close estimated MBL and whole atmosphere CO_2
333 concentrations. In our case, the partitioning of the AGR anomaly in 2015 is not our central purpose. The
334 majority of conclusions reached by our analysis in the paper are based on the inversion-based land carbon
335 uptake anomalies by the two inversion data sets used. Thus we argue the uncertainty of this conversion
336 factor does not significantly impact our results.

337 No revised texts are made in the main text because we think the uncertainty introduced by this factor is
338 minor to the robustness of our conclusion, and because the underlying assumption to use such a factor is
339 already well stated in the text (line 194–195, Page 7).

340 Lines 163-164: What do you mean with “numerical instability”? Why could such an instability happen
341 and why in 1993?

342 [Response] We mean rounding errors that accumulate rather than cancel. We have been experiencing
343 these artifacts more often with increasing assimilation periods over the years, because the grid-point scale
344 inversion problem becomes larger. To our knowledge, there is no particular reason why it happens in
345 1993 rather than in another year. We usually manage to remove these instabilities by re-running the
346 inversion under slightly changed inversion configuration parameters, but this has not been done for this
347 version.

348 Line 296: I thought that the Jena inversion system uses flat land prior fluxes. Are results from the LPJ

349 model really used?

350 [Response] LPJ is used as a time-average spatial pattern, but concerning time variability as relevant here,
351 the CarboScope prior is indeed flat (no prior interannual variations by periodical seasonal variations).

352 Figure 4: The figure could be much easier to read if you do some changes: #1 The red-green colour scale
353 is not needed because the same information is already provided by the x-axis. Additionally, this colour
354 scale might be not visible for colour-blind people. #2 The main purpose of this figure is to compare
355 distributions of seasonal transitions from CAMS and Jena04. Overlaid histograms are not a good
356 graphical choice. I would recommend to rather show distributions in terms of density lines, boxplots or
357 violins which would make it easier to compare the distribution of CAMS and Jena04. The vertical lines
358 for the year 2015 can be still added if you want to keep the focus on this year. #3 Please provide labels
359 and units for the x-axis.

360 [Response] We removed the color in the vertical bars, and changed this plot into line plot of histograms
361 for clarity. Labels and units are provided for x-axis.

362 **14. Are the number and quality of references appropriate?**

363 Yes, but also refer to my answer to the question #7.

364 [Response] We expanded substantially the discussion by citing relevant previous studies. The reference
365 list is updated accordingly.

366 **15. Is the amount and quality of supplementary material appropriate?**

367 Yes, but an improved processing and uncertainty assessment of NDVI data might require more details in
368 the supplementary material.

369 [Response] We provide further figures (Fig. S2, Fig. S3) in the Supplement regarding the 2015 extreme
370 greening.

371 **References**

372 Angert, A., Biraud, S., Bonfils, C., Henning, C. C., Buermann, W., Pinzon, J., Tucker, C. J. and Fung, I.:
373 Drier summers cancel out the CO2 uptake enhancement induced by warmer springs, Proc. Natl. Acad.
374 Sci. U. S. A., 102(31), 10823–7, doi:10.1073/pnas.0501647102, 2005.

375 D’Odorico, P., Gonsamo, A., Pinty, B., Gobron, N., Coops, N., Mendez, E. and Schaepman, M. E.:
376 Intercomparison of fraction of absorbed photosynthetically active radiation products derived from satellite
377 data over Europe, *Remote Sens. Environ.*, 142, 141–154, doi:10.1016/j.rse.2013.12.005, 2014.

378 Fensholt, R. and Proud, S. R.: Evaluation of Earth Observation based global long term vegetation trends
379 — Comparing GIMMS and MODIS global NDVI time series, *Remote Sens. Environ.*, 119, 131–147,
380 doi:10.1016/j.rse.2011.12.015, 2012.

381 Forkel, M., Carvalhais, N., Verbesselt, J., Mahecha, M., Neigh, C. and Reichstein, M.: Trend Change
382 Detection in NDVI Time Series: Effects of Inter-Annual Variability and Methodology, *Remote Sens.*,
383 5(5), 2113–2144, doi:10.3390/rs5052113, 2013.

384 Forkel, M., Carvalhais, N., Rödenbeck, C., Keeling, R., Heimann, M., Thonicke, K., Zaehle, S. and
385 Reichstein, M.: Enhanced seasonal CO₂ exchange caused by amplified plant productivity in northern
386 ecosystems, *Science*, aac4971, doi:10.1126/science.aac4971, 2016.

387 Gonsamo, A., D’Odorico, P., Chen, J. M., Wu, C. and Buchmann, N.: Changes in vegetation phenology
388 are not reflected in atmospheric CO₂ and ¹³C/¹²C seasonality, *Glob. Change Biol.*, n/a- n/a,
389 doi:10.1111/gcb.13646, 2017.

390 Hird, J. N. and McDermid, G. J.: Noise reduction of NDVI time series: An empirical comparison of
391 selected techniques, *Remote Sens. Environ.*, 113(1), 248–258, doi:10.1016/j.rse.2008.09.003, 2009.

392 Holben, B. N.: Characteristics of maximum-value composite images from temporal AVHRR data, *Int. J.*
393 *Remote Sens.*, 7(11), 1417–1434, 1986.

394 Kandasamy, S., Baret, F., Verger, A., Neveux, P. and Weiss, M.: A comparison of methods for smoothing
395 and gap filling time series of remote sensing observations – application to MODIS LAI products,
396 *Biogeosciences*, 10(6), 4055–4071, doi:10.5194/bg-10-4055-2013, 2013.

397 Keenan, T. F., Prentice, I. C., Canadell, J. G., Williams, C. A., Wang, H., Raupach, M. and Collatz, G. J.:
398 Recent pause in the growth rate of atmospheric CO₂ due to enhanced terrestrial carbon uptake, *Nat.*
399 *Commun.*, 7, 13428, doi:10.1038/ncomms13428, 2016.

400 Kern, A., Marjanović, H. and Barcza, Z.: Evaluation of the Quality of NDVI3g Dataset against Collection
401 6 MODIS NDVI in Central Europe between 2000 and 2013, *Remote Sens.*, 8(11), 955,
402 doi:10.3390/rs8110955, 2016.

403 Myneni, R. B., Keeling, C. D., Tucker, C. J., Asrar, G. and Nemani, R. R.: Increased plant growth in the
404 northern high latitudes from 1981 to 1991, *Nature*, 386(6626), 698–702, doi:10.1038/386698a0, 1997.

405 Scheffic, W., Zeng, X., Broxton, P. and Brunke, M.: Intercomparison of Seven NDVI Products over the
406 United States and Mexico, *Remote Sens.*, 6(2), 1057–1084, doi:10.3390/rs6021057, 2014.

407 Thomas, R. T., Prentice, I. C., Graven, H., Ciais, P., Fisher, J. B., Hayes, D. J., Huang, M., Huntzinger, D.
408 N., Ito, A., Jain, A., Mao, J., Michalak, A. M., Peng, S., Poulter, B., Ricciuto, D. M., Shi, X., Schwalm,
409 C., Tian, H. and Zeng, N.: CO₂ and greening observations indicate increasing light-use efficiency in
410 northern terrestrial ecosystems, *Geophys. Res. Lett.*, doi:10.1002/2016GL070710, 2016.

411

412 [References in the response:](#)

413 [Ballantyne, A. P., Alden, C. B., Miller, J. B., Tans, P. P. and White, J. W. C.: Increase in observed net](#)
414 [carbon dioxide uptake by land and oceans during the past 50 years, *Nature*, 488\(7409\), 70–72,](#)
415 [doi:10.1038/nature11299, 2012.](#)

416 [Bastos, A., Ciais, P., Park, T., Zscheischler, J., Yue, C., Barichivich, J., Myneni, R. B., Peng, S., Piao, S.](#)
417 [and Zhu, Z.: Was the extreme Northern Hemisphere greening in 2015 predictable?, *Environ. Res. Lett.*,](#)
418 [12\(4\), 044016, doi:10.1088/1748-9326/aa67b5, 2017.](#)

419 [Ciais, P., Sabine, C., Bala, G., Bopp, L., Brovkin, V., Canadell, J., Chhabra, A., DeFries, R., Galloway, J.,](#)
420 [Heimann, M. and others: Carbon and Other Biogeochemical Cycles, *Clim. Change 2013 Phys. Sci. Basis*](#)
421 [Contrib. Work. Group Fifth Assess. Rep. Intergov. Panel Clim. Change, 465–570, 2014.](#)

422 [Gamon, J. A., Field, C. B., Goulden, M. L., Griffin, K. L., Hartley, A. E., Joel, G., Peñuelas, J. and](#)
423 [Valentini, R.: Relationships Between NDVI, Canopy Structure, and Photosynthesis in Three Californian](#)
424 [Vegetation Types, *Ecol. Appl.*, 5\(1\), 28–41, doi:10.2307/1942049, 1995.](#)

425 [Ide, R., Nakaji, T. and Oguma, H.: Assessment of canopy photosynthetic capacity and estimation of GPP](#)
426 [by using spectral vegetation indices and the light–response function in a larch forest, *Agric. For.*](#)
427 [Meteorol., 150\(3\), 389–398, doi:10.1016/j.agrformet.2009.12.009, 2010.](#)

428 [Myneni, R. B., Keeling, C. D., Tucker, C. J., Asrar, G. and Nemani, R. R.: Increased plant growth in the](#)
429 [northern high latitudes from 1981 to 1991, *Nature*, 386\(6626\), 698–702, doi:10.1038/386698a0, 1997.](#)

430 Prather, M. J., Holmes, C. D. and Hsu, J.: Reactive greenhouse gas scenarios: Systematic exploration of
431 uncertainties and the role of atmospheric chemistry, *Geophys. Res. Lett.*, 39(9), L09803,
432 doi:10.1029/2012GL051440, 2012.

433 Le Quéré, C., Andrew, R. M., Canadell, J. G., Sitch, S., Korsbakken, J. I., Peters, G. P., Manning, A. C.,
434 Boden, T. A., Tans, P. P., Houghton, R. A., Keeling, R. F., Alin, S., Andrews, O. D., Anthoni, P.,
435 Barbero, L., Bopp, L., Chevallier, F., Chini, L. P., Ciais, P., Currie, K., Delire, C., Doney, S. C.,
436 Friedlingstein, P., Gkritzalis, T., Harris, I., Hauck, J., Haverd, V., Hoppema, M., Klein Goldewijk, K.,
437 Jain, A. K., Kato, E., Körtzinger, A., Landschützer, P., Lefèvre, N., Lenton, A., Lienert, S., Lombardozzi,
438 D., Melton, J. R., Metzl, N., Millero, F., Monteiro, P. M. S., Munro, D. R., Nabel, J. E. M. S., Nakaoka,
439 S., O'Brien, K., Olsen, A., Omar, A. M., Ono, T., Pierrot, D., Poulter, B., Rödenbeck, C., Salisbury, J.,
440 Schuster, U., Schwinger, J., Séférian, R., Skjelvan, I., Stocker, B. D., Sutton, A. J., Takahashi, T., Tian,
441 H., Tilbrook, B., Laan-Luijckx, I. T. van der, Werf, G. R. van der, Viovy, N., Walker, A. P., Wiltshire, A.
442 J. and Zaehle, S.: Global Carbon Budget 2016, *Earth Syst. Sci. Data*, 8(2), 605–649, doi:10.5194/essd-8-
443 605-2016, 2016.

444 Tanja, S., Berninger, F., Vesala, T., Markkanen, T., Hari, P., Mäkelä, A., Ilvesniemi, H., Hänninen, H.,
445 Nikinmaa, E., Huttula, T., Laurila, T., Aurela, M., Grelle, A., Lindroth, A., Arneth, A., Shibistova, O. and
446 Lloyd, J.: Air temperature triggers the recovery of evergreen boreal forest photosynthesis in spring, *Glob.*
447 *Change Biol.*, 9(10), 1410–1426, doi:10.1046/j.1365-2486.2003.00597.x, 2003.

448 Zhao, M. and Running, S. W.: Drought-Induced Reduction in Global Terrestrial Net Primary Production
449 from 2000 Through 2009, *Science*, 329(5994), 940–943, doi:10.1126/science.1192666, 2010.

450

451 **Vegetation greenness and land carbon flux anomalies associated with climate**
452 **variations with a focus on the year 2015**

453

454 Chao Yue¹, Philippe Ciais¹, Ana Bastos¹, Frederic Chevallier¹, Yi Yin¹, Christian Rödenbeck²,
455 Taejin Park³

456

457 ¹Laboratoire des Sciences du Climat et de l'Environnement, CEA-CNRS-UVSQ, UMR8212,
458 Gif-sur-Yvette, France

459 ²Max Planck Institute for Biogeochemistry, Jena, Germany.

460 ³Department of Earth and Environment, Boston University, Boston, MA 02215, USA

461

462 Corresponding author: Chao Yue, chao.yue@lsce.ipsl.fr

463

464 **Abstract**

465

466 Enhanced vegetation greening during the past decades over the northern hemisphere was found
467 to be linked with an increasing land sink. In the meantime, interannual variability in the
468 atmospheric CO₂ growth rate is strongly coupled with land carbon uptake dynamics in the
469 tropics, driven by the El Niño–Southern Oscillation (ENSO) climate variations. One may thus
470 wonder how land ecosystems respond to the co-occurrence of extreme greening and an El Niño
471 event. The year 2015 provided an ideal case study for such examination. It was the greenest year
472 since 2000 according to satellite observations of vegetation greenness, but a record atmospheric
473 CO₂ growth rate also happened, associated with a weaker than usual land carbon sink. To
474 reconcile these two observations that may seem paradoxical at first sight, we examined the
475 patterns of large-scale CO₂ fluxes using two atmospheric inversions and the general links among
476 vegetation greenness, seasonal land carbon uptake and climate variations. Inversion results
477 indicate that the year 2015 had a higher than usual northern land carbon uptake in spring and
478 summer, consistent with the greening anomaly. This higher uptake was however followed by a
479 larger source of CO₂ in autumn, suggesting that the extra uptake during the growing season was
480 coupled to and offset by a larger release in the late growing season. Vegetation greenness shows
481 strong positive correlation with land carbon uptake in the northern hemisphere during the

482 growing season, but outside growing season their relation is rather weak. For the tropics and
483 Southern Hemisphere, a strong and abrupt transition toward a large carbon source for the last
484 trimester of 2015 is discovered, concomitant with the El Niño development. This transition of
485 terrestrial tropical CO₂ fluxes between two consecutive seasons is the largest ever found in the
486 inversion records. Although such strong transition to carbon source is consistent with historical
487 observation of a strong dependence of land carbon uptake on tropical temperature and dryness,
488 the detailed underlying mechanisms remain to be elucidated.

489

490 **1 Introduction**

491

492 The first monitoring station for background atmospheric CO₂ concentration was established at
493 Mauna Loa in 1958. Its record shows that atmospheric CO₂ has continued to rise in response to
494 anthropogenic emissions. However, the atmospheric CO₂ growth rate (AGR) has been lower than
495 that implied by anthropogenic emissions alone, because land ecosystems and the oceans have
496 absorbed part of the emitted CO₂ (Canadell et al., 2007; Le Quéré et al., 2016). Although on
497 multi-decadal time scale carbon uptake by land and ocean has kept pace with growing carbon
498 emissions (Ballantyne et al., 2012; Li et al., 2016), large year-to-year fluctuations occur in the
499 terrestrial carbon sink, mainly in response to climate variations induced by El Niño–Southern
500 Oscillation (ENSO) (Wang et al., 2013, 2014) and other occasional events such as volcanic
501 eruptions (Gu et al., 2003). In northern latitude regions, increasing seasonal amplitude of
502 atmospheric CO₂ is found to be linked with an increased land sink, associated with vegetation
503 greening driven partly by long-term warming and CO₂ fertilization (Forkel et al., 2016; Graven
504 et al., 2013; Myneni et al., 1997). The interannual variations in vegetation activity in the northern
505 hemisphere are found to be mainly driven by temperature variations (Piao et al., 2014).

506

507 In 2015, the global monthly atmospheric CO₂ concentration surpassed 400 μmol·mol⁻¹ (ppm) for
508 the first time since the start of background measurements, with an unprecedented large annual
509 growth rate of 2.96±0.09 ppm yr⁻¹
510 (https://www.esrl.noaa.gov/gmd/ccgg/trends/global.html#global_growth). This record-breaking
511 AGR occurred simultaneously with a high value of the ENSO index (Betts et al., 2016) and the
512 warmest land temperature on record since 1880 ([20](https://www.ncdc.noaa.gov/cag/time-</p></div><div data-bbox=)

513 series/global/globe/land/ytd/12/1880-2015). At the same time, 2015 was also shown to have the
514 greenest growing season of the Northern Hemisphere since 2000 (Bastos et al., 2017).
515 Widespread abnormally high positive anomalies of the normalized difference vegetation index
516 (NDVI) were observed from Moderate-resolution imaging spectroradiometer (MODIS) sensor
517 aboard the Terra satellite, in particular over eastern North America and large parts of Siberia. On
518 the one hand, strong greening is expected to enhance northern land carbon uptake during the
519 growing season (Myneni et al., 1997); on the other hand, the strong El Niño event in the second
520 half of 2015 increased fire emissions in tropical Asia (Huijnen et al., 2016; Yin et al., 2016) and
521 likely caused a loss of plant biomass and reduced carbon uptake, possibly associated with the
522 prevailing high temperatures and reduced rainfall (Ahlström et al., 2015; Jiménez-Muñoz et al.,
523 2016).

524

525 To reconcile the observed maximum global land greening with the record-high AGR in 2015, we
526 examined land-atmosphere carbon fluxes estimated from two atmospheric inversions. We
527 [examine the relationship between land carbon uptake anomalies and NDVI anomalies and](#)
528 [climate anomalies, with a special](#) focus on seasonal patterns in the land carbon uptake in 2015
529 relative to the long-term trend of 1981-2015. [The aim here is to infer general patterns in factors](#)
530 [driving the land carbon uptake anomalies and to examine how the carbon dynamics in 2015 fit](#)
531 [into this pattern.](#) We then focus how land ecosystems responded to the joint occurrences of
532 record-breaking warming, extreme greening, and the end-of-year El Niño event, to understand
533 how land ecosystems contributed to the high AGR in 2015.

534

535 **2 Data and methods**

536 **2.1 Data sets**

537 **2.1.1 Atmospheric inversion data**

538 We used two gridded land and ocean carbon uptake data sets based on atmospheric CO₂
539 observations, namely those from the Copernicus Atmosphere Monitoring Service (CAMS)
540 inversion system developed at LSCE (Chevallier et al., 2005, 2010) and from the Jena
541 CarboScope inversion system developed at the MPI for Biogeochemistry Jena (update of
542 Rödenbeck, 2005; Rödenbeck et al., 2003). Atmospheric inversions estimate land- and ocean-
543 atmosphere net carbon fluxes by minimizing a Bayesian cost function, which accounts for the

544 mismatch between observed and simulated atmospheric CO₂ mixing ratios. To do this, they use
545 atmospheric CO₂ concentration at observation sites, combined with an atmospheric transport
546 model as well as prior information on carbon emissions from fossil fuel burning and on carbon
547 exchange between the atmosphere and land (and ocean). Detailed information inversions could
548 be found in respective sources as mentioned above.

549

550 The CAMS inversion data (version r15v3) were provided for 1979-2015 with a weekly time-step
551 and a spatial resolution of 1.875° latitude and 3.75° longitude. The Jena CarboScope inversion
552 provides daily fluxes at a spatial resolution of 3.75° latitude and 5° longitude. It offers a series of
553 runs that use differently large station sets with complete data coverage over time, in order to
554 avoid spurious flux variations from a changing station network. From these runs, we used
555 s04_v3.8 (shortened as Jena04 in the main text and supplementary material) using the largest
556 number of measurement sites and therefore the most detailed constraint on carbon exchanges in
557 2015 (see <http://www.bgc-jena.mpg.de/CarboScope/> for more details on other configurations).
558 The s04_v3.8 run has a validity period as 2004–2015, although it does provide the data for the
559 whole time span of 1981–2015. [Site observations used over the validity period are coherent over
560 time and it is optimal to examine the temporal trend within such a period. But results outside the
561 validity period are still technically feasible and the temporal trend could thus be examined over
562 the whole entire time span.](#) We compared the linear trends over the larger latitudinal regions
563 examined in this study between the s04_v3.8 and the long s81_v3.8 runs, and confirmed that the
564 derived trends are similar. Therefore, in the calculation of the long-term linear trend used as a
565 reference of interannual anomalies (see Sect. 2.2.2 below), we exceptionally use the s04_v3.8
566 run outside its period of validity. [The CAMS inversion uses sites with at least 5-year worth of
567 data. It therefore has a denser \(during the recent decade\) but temporally evolving data coverage
568 than Carboscope. The evolving network in CAMS causes changes in inverted CO₂ fluxes that are
569 superimposed on changes from biogeochemical drivers during the whole period.](#)

570

571 In order to compare with the inversion data, land and ocean net carbon uptakes for 1981–2015
572 from the Global Carbon Project (Le Quéré et al., 2016) were used. For this purpose, an annual
573 global carbon flux of 0.45 Pg C yr⁻¹ is subtracted from the inversion-derived land carbon uptakes
574 and is added to ocean carbon uptakes to account for the pre-industrial land-to-ocean carbon

575 fluxes induced by river transport (Jacobson et al., 2007), following Le Quéré et al. (2016).
576 Estimates of ocean carbon uptake in GCP are based on observation-based mean CO₂ sink
577 estimate for the 1990s and variability in the ocean CO₂ sink for 1959–2015 from global ocean
578 biogeochemistry models. Estimates of land carbon uptake in GCP are calculated as the difference
579 between anthropogenic emissions, atmospheric CO₂ growth and ocean sink. The estimates of
580 land and ocean carbon uptake in GCP are largely independent from the two inversions used here,
581 except that the CO₂ records from atmospheric stations which are used in inversions are also used
582 in GCP to derive global AGR.

583

584 **2.1.2 Atmospheric CO₂ growth rates, NDVI and climate data**

585 Atmospheric CO₂ growth rates were retrieved from the Global Monitoring Division, Earth
586 System Research Laboratory (ESRL), NOAA
587 (<http://www.esrl.noaa.gov/gmd/ccgg/trends/global.html>). We used NDVI data between 2000 and
588 2015 from MODIS Terra Collection 6 (Didan, 2015), on a resolution of 0.05° and 16-day time
589 step. NDVI data is processed from MODIS land surface reflectance data and thoroughly
590 corrected for atmospheric effects. We strictly applied quality assurance (QA) controls to
591 maintain distinct seasonal trajectory of vegetative radiometric observations and minimize
592 spurious signals (e.g., snow or cloud). Detected unexpected non-vegetative observations were
593 first excluded and then filled by the adaptive Savitzky–Golay filter (Chen et al., 2004; Jönsson
594 and Eklundh, 2004). The Savitzky–Golay filter is a simplified convolution over a set of
595 consecutive values with weighting coefficients given by a polynomial least-square-fit within the
596 filter window (Savitzky and Golay, 1964). After this procedure, the linearly interpolated daily
597 NDVI data was used to calculate mean seasonal NDVI and re-gridded at 0.5° resolution, with
598 pixels of seasonal NDVI lower than 0.1 being further masked to ensure robustness. We examined
599 four seasons: Q1 (January–March), Q2 (April–June), Q3 (July–September) and Q4 (October–
600 December). Climate fields are from the ERA interim reanalysis (Dee et al., 2011) at 0.5°
601 resolution and monthly time-step. We used air temperature, precipitation and volumetric soil
602 water content (%) integrated over the soil column to a depth of 2.89 m.

603

604 **2.1.3 Indices for El Niño–Southern Oscillation (ENSO) states and fire emission data**

605 We examined the seasonal variations of the carbon cycle in 2015 in relation to ENSO events and

606 compared the 2015 El Niño event with that of 1997–1998. The Multivariate ENSO Index (MEI,
607 <http://www.esrl.noaa.gov/psd/enso/mei/>, Wolter and Timlin, 2011) was used to indicate the
608 ENSO state. MEI is a composite index calculated as the first un-rotated principal component of
609 six ENSO-relevant variables (including sea level pressure and sea surface temperature) over the
610 tropical Pacific for each of the twelve sliding bi-monthly seasons. MEI was widely used in
611 previous studies as an indicator for ENSO states to examine land carbon dynamics (Nemani et
612 al., 2003; van der Werf et al., 2008). The 12 bi-monthly MEI values of each year are summed to
613 obtain the annual MEI. The interannual variations in climate and land carbon uptake are linked
614 with MEI to infer general relationship between land carbon dynamics and ENSO climate
615 oscillations. To examine the potential role of fire emissions in the land carbon balance in 2015,
616 we used the GFED4s carbon emission data at daily time-step and 0.25° spatial resolution
617 (<http://www.globalfiredata.org/data.html>). Monthly fire-carbon emissions were calculated for the
618 regions and were examined for 1997–2015.

619

620 **2.2 Data analysis**

621 **2.2.1 NDVI rank analysis and greening trend**

622 Given a season and a pixel, the annual time series of seasonal NDVI for 2000-2015 were ranked
623 in ascending order so that each year could be labelled by a rank, with 1 being the lowest and 16
624 being the highest. A spatial map of NDVI rank was then obtained for each year for the given
625 season (Fig. S1). A composite map was made for year 2015, by merging pixels with the highest
626 rank of all four seasons in 2015 (Fig. 1a). Vegetated area fraction with the highest rank for
627 different years was obtained, with the sum of these fractions yielding unity. This procedure was
628 repeated for all four seasons to generate four seasonal time series, with each containing the
629 vegetation land fractions with highest NDVI for different years (Fig. 1b). It is noted that NDVI
630 values for the northern hemisphere for Q1 and Q4 mostly fall outside the growing season
631 (although October is frequently considered within the growing season and some evergreen
632 coniferous forests show significant photosynthetic activities in March in regions of mild winter,
633 e.g., Tanja et al., 2003), so that a valid NDVI might not necessarily be associated with significant
634 seasonal vegetation activity. But as we applied a minimum value of 0.1 on seasonal NDVI, we
635 expect that this issue is partly alleviated. Such seasonal segregation is adopted mainly because of
636 its general applicability across the globe, especially for tropical ecosystems where seasonality in

637 [vegetation activities is minimal.](#)

638

639 **2.2.2 Analysis of land carbon uptake dynamics associated with climate variations**

640 Annual land and ocean carbon uptakes and carbon emissions from the two inversions were
641 calculated for the globe over their period of overlap, 1981–2015. AGRs from NOAA/ESRL over
642 1981–2015 were converted into Pg C using a conversion factor of 2.12 Pg C ppm⁻¹ (Ballantyne
643 et al., 2012; Prather et al., 2012; Quéré et al., 2016) to examine the closure of the global carbon
644 balance. The conversion factor used here assumes that the entire atmosphere is well mixed
645 within one year. Because the record high AGR in 2015 was a composite effect collectively
646 determined by carbon emissions from fossil fuel burning and industry, and land and ocean
647 carbon uptakes, all being impacted by a historical trend (Fig. 2), [it thus must be put into an](#)
648 [historical perspective to reconcile evidence for extreme greening and the highest atmospheric](#)
649 [CO₂ growth rate. For example, if 2015 comes up with a large increase in carbon emissions](#)
650 [accompanied by droughts \(browning\) in the northern hemisphere and the tropics, then the highest](#)
651 [AGR might not be regarded as a big surprise. Therefore, to understand the contributing factors](#)
652 [for the highest AGR in 2015, we separated it into a long-term trend and interannual anomalies.](#)
653 For this reason, annual time series of carbon emissions, land and ocean carbon uptakes, and
654 AGRs from NOAA/ESRL over 1981–2015 were linearly de-trended. The percentages of
655 anomalies in carbon emissions, land and ocean sink in 2015 to the 2015 AGR anomaly were then
656 calculated as relative contributions by each factor to the 2015 AGR anomaly.

657

658 Seasonal land carbon uptake anomaly time series were also calculated (the 0.45 Pg C yr⁻¹ annual
659 correction was not applied) by subtracting the same linear trend for 1981–2015. The globe was
660 divided into three latitude bands: boreal Northern Hemisphere (BoNH, latitude > 45°N),
661 temperate Northern Hemisphere (TeNH, 23.5° < latitude < 45°N), and tropics and extratropical
662 Southern Hemisphere (TroSH, latitude < 23.5°N). The BoNH and TeNH are grouped as Boreal
663 and temperate Northern Hemisphere (BoTeNH, latitude > 23.5°N) when examining seasonal
664 carbon transitions. Seasonal land carbon uptake anomalies are then calculated for each region
665 and the whole globe, with positive anomalies indicating enhanced sink (or reduced source)
666 against the linear trend (i.e., the normal state), and negative ones indicating the opposite. The
667 same seasonal linear de-trending was also performed for climate fields of air temperature,

668 precipitation and soil water content. The relationship between anomalies in land carbon uptake,
669 temperature and precipitation are then examined using partial correlation coefficients in a
670 multivariate linear regression framework with an ordinary least squares method. The relationship
671 between seasonal land uptake anomalies and NDVI anomalies are also examined using simple
672 linear regression.

673
674 We then examined especially the seasonal anomalies of land carbon uptake in 2015 and the
675 carbon uptake transitions between two consecutive seasons, trying to reconcile extreme greening
676 and a moderate land sink for this year. Seasonal land carbon uptake transitions are calculated as
677 the land sink anomaly in a given season minus that of the previous one. When examining
678 transitions of land carbon uptake anomalies by the CAMS inversion, we found the year 1993 has
679 an extreme negative Q3→Q4 global transition (-2.85 Pg C within 6 months, $< -4\sigma$, the second
680 lowest being the year 2015 with -1.0 Pg C) albeit with a reasonable annual land carbon uptake
681 ($3.75 \text{ Pg C yr}^{-1}$). This is linked with an extreme high Q3 and low Q4 uptake in this year, which
682 could not be explained by any known carbon cycle mechanisms. This is thus identified as a result
683 of numerical instability of the inversion system for that release and consequently the year 1993
684 has been removed from all the aforementioned seasonal analyses.

685

686 **3 Results**

687 **3.1 Vegetation greening in 2015**

688 Figure 1a illustrates where and when higher-than-normal greening conditions were observed in
689 different seasons of the year 2015, compared to other years of 2000–2015 (see Supplementary
690 Fig. S1 for greenness distribution for each season). On average over the four seasons of 2015,
691 16% of vegetated land shows record seasonal NDVI. The year with the second highest NDVI is
692 2014 with 9% vegetated area having record NDVI. An increase of the record-breaking NDVI
693 occurrence over time is clearly seen in Fig. 1b. In short, 2015 clearly stands out as a greening
694 outlier, having the highest proportion of vegetated land being the greenest for all four seasons
695 except for the first season (despite the fact that for Q1, 2015 is still the third highest, Q1 =
696 January to March).

697

698 For boreal and temperate regions of the Northern hemisphere, the seasons with highest NDVI in

699 2015 are dominated by Q2 and Q3 (Q2 = April to June; Q3 = July to September), corresponding
700 to the growing season from spring to early autumn (Supplementary Fig. S2). A pronounced
701 greening anomaly in Q2 occurred in western to central Siberia, western Canada and Alaska, and
702 eastern and southern Asia (Supplementary Fig. S1). Central and eastern Siberia and eastern
703 North America showed marked greening in Q3. Strong and widespread greening also occurred in
704 the tropics during Q3 over Amazonia and the savanna (or cerrado) of eastern South America and
705 tropical Africa, but this strong positive greening signal greatly diminished in Q4 (Q4 = October
706 to December) especially over central to eastern Amazonia with the development of El Niño
707 (Supplementary Fig. S1). The strongest greening in 2015 across the globe is overall dominated
708 by the northern land (latitude > 23.5°N), while for the northern tropics (0–23.5°N) only
709 moderately strong greening is found, and for the southern hemisphere the greening of 2015 is
710 close to the average state of the period of 2000–2015 (Supplementary Fig. S3). The extreme
711 growing-season greening in the northern land is confirmed by Bastos et al. (2017) as robust by
712 using Terra MODIS NDVI data with different quality control procedures, and consistent between
713 Terra and Aqua sensors (Fig. S1 in Bastos et al., 2017).

714

715 **3.2 Global carbon balance for 1981-2015**

716 Figure 2 shows the time series of fossil and industry carbon emissions, NOAA/ESRL AGR rates
717 linked with ENSO climate oscillations as indicated by the Multivariate ENSO Index (MEI), and
718 land and ocean carbon sinks for the common period of the two inversions (1981–2015) and the
719 estimates by the Global Carbon Project (GCP). Emissions show a clear increase with time,
720 however AGRs are more varying. The record high AGR of 2.96 ppm in 2015 exceeds those in all
721 other previous years including the extreme El Niño event in 1997–98 despite much higher annual
722 emissions in 2015. Interannual variability in AGR is mainly caused by fluctuations in land
723 carbon sink, with Pearson's correlation coefficients between de-trended AGR and land sink < -
724 0.8 ($p < 0.01$) for both inversions (Pearson's correlation coefficient between de-trended AGR and
725 MEI being 0.27, $p < 0.1$). The root mean square differences between inversion and GCP carbon
726 sinks are 0.70 and 0.65 Pg C yr⁻¹ for CAMS and Jena04 respectively for the land, and ~0.5 PgC
727 yr⁻¹ for the ocean for both inversions, within the uncertainties of 0.8 and 0.5 Pg C yr⁻¹ over 1981–
728 2015, respectively for land and ocean as reported by GCP. The interannual variability of de-
729 trended sink anomalies for the land agrees well between inversions and GCP (with Pearson's

730 correlation coefficient being 0.9 for both inversions, $p < 0.01$).

731

732 For 2015, the prescribed anthropogenic carbon emissions in the CAMS inversion are 9.9 Pg C yr^{-1} ,
733 of which 2.0 Pg C are absorbed by ocean, 1.7 Pg C by land ecosystems, with 6.2 Pg C
734 remaining in the atmosphere, which matches the AGR from background stations of 6.3 Pg C
735 assuming a conversion factor of $2.12 \text{ Pg C ppm}^{-1}$ (Ballantyne et al., 2012; Le Quéré et al., 2016)
736 and considering a measurement uncertainty of AGR as 0.09 ppm (0.2 Pg C) for 2015. When land
737 carbon fluxes from the inversion are linearly de-trended over 1981-2015, the terrestrial sink in
738 2015 is by 1.2 Pg C lower than normal (i.e., the trend value), but this is not an extreme value —
739 it is only the seventh weakest sink since 1981. This weaker land uptake accounts for 82% of the
740 positive AGR anomaly, which is 1.45 Pg C in 2015 by subtracting a linear temporal trend.
741 Jena04 yields an AGR in 2015 that is 0.13 ppm lower than the AGR based on background
742 stations only, a difference close to the observation uncertainty. After removing the linear trends
743 over time similarly as for the CAMS inversion, the land carbon uptake anomaly for Jena04 is -
744 0.3 Pg C yr^{-1} in 2015, or 20% of the observed AGR anomaly, the remaining being explained by a
745 positive anomaly in fossil fuel emissions (34%), a negative anomaly in the ocean sink (20%),
746 and the difference between modelled AGR and NOAA/ESRL reported AGR. Note that the land
747 sink by GCP for 2015 is much lower than in the two inversions, with de-trended anomaly lower
748 than that of CAMS, indicating even larger contribution from land to the high anomaly of AGR.

749

750 In general, the warm phases of ENSO events are associated with positive anomalies in land air
751 temperature, negative precipitation anomalies, and lower land carbon uptake anomalies (Fig. 3),
752 consistent with previous studies (Cox et al., 2013; Wang et al., 2014). The lower precipitation
753 during El Niño is due to a shift of precipitation from tropical land to the ocean (Adler et al.,
754 2003), and higher land temperature might be due to reduction in evaporative cooling. The two
755 extreme El Niño years of 1997 and 2015 have rather close MEI values. Compared with the
756 ‘standard’ El Niño state of temperature and precipitation represented by the regression line, the
757 year 1997 was relatively ‘cool’ and ‘wet’, while 2015 was rather ‘warm’ and ‘dry’ (with an
758 extremely negative precipitation anomaly). Year 1998 has a smaller value of MEI than
759 1997/2015, but has a higher temperature anomaly than 2015, and a much lower land carbon
760 uptake anomaly than 1997 and 2015 in both inversions, while the land carbon uptake anomalies

761 in 1997 and 2015 are similar. More detailed comparison of these three years and their carbon
762 cycle dynamics will be presented in the discussion section.

763

764 **3.3 Seasonal land carbon uptake dynamics associated with climate variations with a focus** 765 **on 2015**

766

767 The partial correlation coefficients between anomalies in seasonal land carbon uptake and those
768 in seasonal temperature and precipitation for different regions are shown in Fig. 4. The simple,
769 individual (univariate) linear relationships between de-trended anomalies in land carbon fluxes
770 and those in temperature and precipitation, are presented in Supplementary Fig. S4 and S5. Land
771 carbon fluxes show consistent relationships with temperature between the two inversions for
772 BoNH: positive relationship for Q2 and a negative one for the other three seasons (with Q1 by
773 Jena04 being the only insignificant one). Partial correlations between land fluxes and
774 precipitation are absent or non-significant for BoNH. This points to the fact that vegetation
775 productivity in BoNH is in principle dominated by temperature, with warmer spring and early
776 summer (Q2, April–June) enhancing vegetation net carbon uptake, but a higher temperature in
777 later summer, autumn and early winter mainly reduces the land capacity to sequester carbon,
778 consistent with previous studies (Piao et al., 2008). For TeNH, a significant negative relationship
779 is found between land fluxes by the CAMS inversion and temperature for Q3, and both
780 inversions show negative relationship between land fluxes and precipitation for Q4, probably due
781 to enhanced early autumn respiration under wetter conditions. For TroSH, land carbon uptakes in
782 Q1, Q2 and Q4 are all negatively related with temperature ($p < 0.05$ for both inversions), while
783 increase in precipitation in Q1 is found to be associated with enhanced land uptake.

784

785 To explain the seeming paradox in 2015 between the strong greening and an only moderate
786 terrestrial uptake, we examined in detail the seasonal land carbon flux anomalies in 2015 (Fig. 5,
787 refer to Supplementary Fig. S6 for the spatial distribution of flux anomalies). At seasonal scale,
788 both inversions indicate positive carbon uptake anomalies during Q2 and Q3 for boreal and
789 temperate Northern Hemisphere (BoTeNH, latitude $> 23.5^\circ\text{N}$), consistent with marked greening
790 in central to eastern Siberia, eastern Europe and Canada (Fig. 1) as outlined above. **Indeed, both**
791 **BoNH and TeNH show positive relationships between seasonal land carbon flux anomalies and**

792 NDVI anomalies for Q2 and Q3, with BoNH showing moderate greenness (after a linear trend
793 being removed) for Q3 and TeNH showing extreme greenness for Q2 in 2015 (Supplementary
794 Fig. S7). However, an extreme follow-up negative (source) anomaly occurred in Q4 (Fig. 5a).
795 These negative anomalies were lower than the 10th percentile of all anomalies in Q4 over time
796 for both inversions and they partly cancelled the extra uptake in Q2 and Q3. As a result, on the
797 annual time scale, the CAMS inversion shows an almost neutral land flux anomaly in BoTeNH,
798 while the Jena04 inversion still indicates a significant positive annual anomaly.

799
800 For the tropics and extratropical Southern Hemisphere (TroSH, latitude < 23.5°N), both
801 inversions show a weak negative land carbon anomaly for Q1 (mean value of -0.10 Pg C) in
802 2015, moderate anomalies in Q2 (of differing signs, with a negative one of -0.3 Pg C in CAMS
803 and a positive one of 0.2 Pg C in Jena04). Q3 anomalies are almost carbon neutral for both
804 inversions. In stark contrast, between Q3 and Q4, both inversions show a strong shift toward an
805 abnormally big land carbon source (i.e., negative anomalies of ~ -0.7 Pg C against a carbon
806 source expected from the linear trend, lower than 10th percentile over time in both inversions).
807 On the annual time scale, CAMS shows a large negative anomaly of -1.2 Pg C. For Jena04, sink
808 and source effects in Q1–Q3 cancelled each other, leaving the annual anomaly the same as in Q4.

809
810 Over the globe, the Jena04 inversion shows an abnormally strong sink during Q2 (normal state
811 being a net carbon sink), owing to synergy of enhanced Q2 uptakes in both BoTeNH and TroSH.
812 This abnormally enhanced uptake partly counteracted the strong shift toward source in Q4
813 (normal state being a net carbon source), leaving a small negative annual land carbon balance of
814 -0.3 Pg C. For the CAMS inversion, because of the co-occurrence of enhanced carbon release in
815 BoTeNH and the sudden shift toward a large carbon source in TroSH both in Q4 (normal states
816 being both net carbon sources), the land shows a strong global shift toward being a source in Q4,
817 leaving a negative annual carbon anomaly of -1.2 Pg C (i.e., carbon sink being reduced
818 compared with the normal state).

819
820 These consistent results from both inversions point to very strong seasonal shifts in the land
821 carbon balance as an emerging feature of 2015. We thus calculated *transitions* in land carbon
822 uptake anomaly as the first-order difference in flux anomalies between two consecutive seasons

823 (defined as the anomaly in a given season minus that in the previous one) for all years of the
824 period 1982-2015 (Fig. 6). The ranks of transitions for different seasons relative to other years
825 between the two inversions are broadly similar, except for Q1→Q2 and Q2→Q3 in TroSH,
826 mainly due to the differences between the two inversions in seasonal land-carbon uptake
827 anomaly in Q2 (Fig. 5b). On the global scale, both inversions show an extreme transition to a
828 negative uptake anomaly for Q3→Q4, with 2015 being the largest transition of the period 1982-
829 2015 (a transition towards an enhanced carbon source of -1.0 Pg C in 6 months). The abnormal
830 transitions for Q3→Q4 on the global scale are located in the TroSH region, where both
831 inversions show that during 1982-2015 the largest transition occurred in 2015. For BoTeNH,
832 both inversions showed strong transitions toward positive anomaly for Q1→Q2; however, the
833 same strong transition toward source anomaly occurred in Q3→Q4, partly cancelling the sink
834 effects during growing seasons.

835

836 **4 Discussion**

837 **4.1 Land carbon uptake dynamics with climate variations in northern latitudes and** 838 **seasonal transitions of land carbon uptakes in 2015**

839 The two inversions consistently allocate a strong positive carbon uptake anomaly in the region of
840 BoTeNH during spring, which persists through the summer (Q2–Q3): an extreme sink anomaly
841 is estimated in Q2 by Jena04, but a more moderate one by CAMS (still above the 75th
842 percentile). The strong sinks in Q2 in both inversions are dominated by temperate Northern
843 Hemisphere regions (TeNH, $23.5^\circ < \text{latitude} < 45^\circ\text{N}$, Supplementary Fig. S8). [For this region,](#)
844 [both inversions show strong positive correlation between carbon uptake anomalies and NDVI in](#)
845 [Q2, with an extremely high NDVI anomaly in 2015 \(Supplementary Fig. S7f\).](#) Therefore, the
846 [strong sinks in Q2 are evidently linked with the extreme greening, although temperature and](#)
847 [precipitation are only moderate \(Fig. S4f, Fig. S5f\).](#)

848

849 For Q3, an extreme carbon sink anomaly occurs in boreal Northern Hemisphere (BoNH,
850 $\text{latitude} > 45^\circ\text{N}$) in CAMS; however, an equally strong negative anomaly (i.e., reduced sink) was
851 found in TeNH in the same season, leaving the whole boreal and temperate Northern
852 Hemisphere (BoTeNH) only a moderately enhanced sink anomaly (Fig. S8). Thus for TeNH
853 alone, CAMS indicates extreme seasonal shift from a positive anomaly in Q2 to a negative one

854 in Q3, implying abrupt seasonal transitions probably resulting from enhanced ecosystem CO₂
855 release after growing-season uptake. For TeNH in 2015, NDVI persisted from a high extreme in
856 Q2 to high values in Q3 (Fig. S7), and temperature remained moderate for both Q2 and Q3 (Fig.
857 S4f, S4g), but precipitation shifted from a moderate anomaly in Q2 to an extremely low one (Fig.
858 S5f, S5g). Therefore, the shift from a high Q2 sink anomaly to a big Q3 source anomaly by
859 CAMS might be partly linked with the shift in precipitation and drought in Q3, such as the
860 prevailing drought in Europe as shown in Fig. S9 (see also a detailed discussion of the European
861 drought in Orth et al., 2016).

862

863 Inversion Jena04 agrees with a higher-than-normal sink in TeNH ($23.5^\circ < \text{latitude} < 45^\circ\text{N}$)
864 during spring (Q2). It also reports a moderate positive anomaly for Q3 in BoNH, but does not
865 show a strong negative anomaly (i.e., reduced sink) in TeNH in Q3 as CAMS does (Fig. S8).
866 This is possibly related to differences in the measurement station data used, to different land
867 prior fluxes (from the ORCHIDEE model in CAMS, and the LPJ model in Jena CarboScope), or
868 to the fact that Jena inversion has a larger a-priori spatial error correlation length scale for its
869 land fluxes (1275 km) than CAMS (500 km) (Chevallier et al., 2010; Rödenbeck et al., 2003).
870 Nonetheless, both inversions consistently indicate that the enhancement of CO₂ uptake during
871 spring and summer at the northern hemispheric scale was subsequently offset by an extreme
872 source anomaly in autumn (Q4).

873

874 The large carbon source anomalies in Q4 shown by the two inversions in BoTeNH seem to be
875 dominated by different factors in BoNH versus TeNH. In BoNH the source anomaly in 2015 is
876 more linked with elevated temperature in Q4, which shows significant negative correlations with
877 carbon uptake anomalies by both inversions (Fig. S4d). In contrast, precipitation in Q4 has no
878 correlation with carbon uptake anomalies, and precipitation in 2015 was close to the normal state
879 (Fig. S5d). The prevailing high temperature in Q4 of 2015 is especially evident over most of
880 northern America, and central to eastern Siberia and Europe (Supplementary Fig. S9a).

881

882 In TeNH, the roles of temperature and precipitation are reversed compared to BoNH. Q4
883 precipitation is found to have significant negative correlation with land carbon uptake anomalies
884 for both inversions, and Q4 in 2015 was characterized by a very high precipitation anomaly,

885 leading to reduced land carbon uptake (Fig. S5h). While temperature in Q4 of 2015 was
886 moderately high, no significant correlation is found between carbon uptake anomalies and
887 temperature (Fig. S4h). However, for both BoNH and TeNH, NDVI remained moderately high
888 in Q4 of 2015 (Fig. 7d, 7h).

889
890 The positive relationship between land carbon uptake and temperature in Q2 (spring and early
891 summer), and a negative one for Q3 and Q4 (autumn) for BoNH, are in line with previous
892 studies. Several studies reported an enhanced greening during spring and summer in the northern
893 hemisphere (Myneni et al., 1997; Zhou et al., 2001), as driven by increasing spring and summer
894 temperature (Barichivich et al., 2013; Nemani et al., 2003), leading to enhanced land carbon
895 uptake and a long-term increase in the seasonal amplitudes of atmospheric CO₂ in northern
896 latitudes (Forkel et al., 2016; Graven et al., 2013). However, for autumn, even though growing
897 season in autumn has been delayed because of autumn warming (Barichivich et al., 2013), land
898 carbon uptake termination time is found to have advanced as well, mainly due to enhanced
899 autumn respiration (Piao et al., 2008), which ultimately reduced net ecosystem carbon uptake
900 (Hadden and Grelle, 2016; Ueyama et al., 2014). For TeNH, we also found significant negative
901 relationship between land carbon uptake anomalies and temperature for Q3 using the CAMS
902 inversion data, consistent with the enhanced respiration by autumn warming found in
903 aforementioned studies. For Q4, however, both inversions point to decreasing land carbon
904 uptakes with increasing precipitation. This might be due to enhanced respiration by ameliorated
905 soil moisture condition, but this finding needs further examination on site scale in future studies.

906
907 For BoNH and TeNH, land carbon uptake anomalies are closely coupled with NDVI anomalies
908 for Q2 (positive correlation, albeit an insignificant one for TeNH Q2 using Jena04 data), but they
909 are generally de-coupled for Q3 and Q4, except that for Q3 of BoNH the CAMS-based land
910 carbon uptake show positive correlation with NDVI. This suggests high NDVI in autumn might
911 not necessarily relate to a high land carbon uptake. This is mainly because of two reasons. First,
912 NDVI is found to correlate well with leaf-level CO₂ uptake for deciduous forest for different
913 seasons, but is largely independent of leaf photosynthesis for evergreen forests (Gamon et al.,
914 1995). Second, even though a higher NDVI is associated with larger photosynthetic capacity and
915 a higher gross photosynthesis, autumn warming might increase ecosystem respiration more than

916 photosynthesis, leaving still a net carbon source effect. Furthermore, other studies also pointed
917 out that severe summer drought can negate the enhanced carbon uptake during warm springs
918 (Angert et al., 2005; Wolf et al., 2016).

919

920 **4.2 Seasonal land carbon uptake transitions in the tropics and influences of El Niño and** 921 **vegetation fire**

922

923 The strong transition to abnormal source in the tropics and extratropical Southern Hemisphere
924 was paralleled by a marked decrease in precipitation and an increase in temperature in Q4, with
925 the development of El Niño in Q2–Q3 (Supplementary Fig. S4I, S5I, S10). Here El Niño
926 development is indicated by the rise of the MEI and Oceanic Niño Index (ONI,
927 http://www.cpc.ncep.noaa.gov/products/analysis_monitoring/ensostuff/ONI_change.shtml). This
928 strong transition is consistent with the expected response of tropical and sub-tropical southern
929 ecosystems during previous El Niño events (Ahlström et al., 2015; Cox et al., 2013; Poulter et
930 al., 2014; Wang et al., 2013, 2014). The small abnormal source in Q1 in TroSH is consistent with
931 a low precipitation anomaly. While temperature anomalies are abnormally high in Q2 and Q3,
932 accompanied by extremely negative precipitation anomalies, the extremely low carbon flux in
933 Q4 is largely explained by temperature, because correlations between land carbon uptake and
934 precipitation in Q4 are very weak (Fig. S4i–l, Fig. S5i–l). Vegetation greenness has significant
935 positive correlation with land carbon uptake anomalies for only Q1 in the tropics, and for the rest
936 three seasons the correlation is very weak (Fig. S7i–l).

937

938 Compared with the 1997–98 El Niño, which was of similarly extreme magnitude, the 2015 El
939 Niño started much earlier with positive MEI and ONI appearing during the first half of 2014.
940 Since then until Q3 and Q4 in 2015 when El Niño began to reach its peak, the tropics and
941 Southern Hemisphere saw continuous higher-than-normal temperatures, with continually
942 decreasing precipitation and accumulating deficit in soil water content (Supplementary Fig. S10).
943 From Q3 to Q4, a steep decline is further observed in both precipitation and soil moisture with
944 stagnating high temperature anomaly, which is probably a major cause of the strong shift toward
945 a carbon source anomaly. The CAMS inversion shows a carbon source anomaly in Q4 of 2015
946 slightly smaller than that in Q3 of 1997, while the Jena04 inversion shows almost equal

947 magnitudes of loss in land sink strength between these two extreme El Niño events. On the one
948 hand, El Niño in late 2015 started with an early onset and built upon the cumulative effects of the
949 drought since the beginning of the year; it thus came with larger negative anomaly in
950 precipitation and soil water content than the 1997–98 El Niño. This sequence of events might
951 favour a stronger land carbon source. On the other hand, the fire emission anomaly in the tropics
952 in 2015 was less than half of that in 1997 at the peak of El Niño (Fig. S10), which might
953 contribute to a smaller land source anomaly in 2015 than in 1997–98.

954
955 El Niño events are usually associated with increased vegetation fires, and these have a large
956 impact on the global carbon cycle (van der Werf et al., 2004). Global fire emissions of carbon
957 reached 3.0 and 2.9 Pg C in 1997 and 1998 according to the GFED4s data. These two years
958 produced the largest source of fire-emitted carbon for the entire period 1997–2015. Global fire
959 emissions in 2015 reached 2.3 Pg C, close to the 1997–2015 average (2.2 Pg C yr⁻¹) but 23–24%
960 lower than 1997–98 — the difference mainly occurring in the southern tropics (0–23.5°S, Fig.
961 S10). In particular, carbon emissions from deforestation and peat fires were two times lower in
962 2015 (0.6 Pg C) compared with 1997 (1.2 Pg C) (GFED4s data), and emissions for these types of
963 fires are more likely to be a net source contribution, because they cannot be compensated by
964 vegetation regrowth within a short time. Fire emission data thus suggests a smaller contribution
965 from fires to AGR in 2015 than 1997–98. If both annual time series of AGR and global fire-
966 carbon emissions are de-trended within their overlapping period of 1997–2015, fire-carbon
967 emissions have an anomaly of 0.4 Pg C yr⁻¹ in 2015, explaining only 29% of the AGR anomaly.

968
969 There has been a long debate on whether tropical vegetations show enhanced greenness as
970 indicated by vegetation indices (i.e., NDVI and enhanced vegetation index or EVI) during dry
971 seasons or drought periods in tropical forest (Huete et al., 2006; Morton et al., 2014; Saleska et
972 al., 2007; Samanta et al., 2010; Xu et al., 2011), and whether there is an accompanying decrease
973 in long-term vegetation productivity associated with droughts (Medlyn, 2011; Samanta et al.,
974 2011; Zhao and Running, 2010). Some studies show enhanced green-up in Amazonian forest
975 during dry seasons mainly due to the release of radiation control on vegetation activities (Huete
976 et al., 2006; Zhao and Running, 2010), while Samanta et al. (2010) argued such observed green-
977 up is an artefact of atmosphere-corrupted data. A recent study by Morton et al. (2014) rather

978 argued that if errors of satellite observation angle are corrected, no increase in EVI could be
979 observed during dry seasons.

980

981 While forest plot level data demonstrated consistent negative effect of droughts on tropical
982 carbon uptake mainly through enhanced tree mortality (Lewis et al., 2011; Phillips et al., 2009),
983 site level observations failed to see immediate reduction in forest net primary productivity
984 (Doughty et al., 2015) or even saw increased gross photosynthesis or photosynthesis capacity
985 when dry seasons initiate (Huete et al., 2006; Wu et al., 2016). Further, a large mortality event
986 for trees will cause a legacy source over several years rather than a rapid release of CO₂ to the
987 atmosphere during the year when trees died.

988

989 Both Wang et al. (2013) and Wang et al. (2014) found a higher correlation coefficient between
990 interannual variability in tropical land carbon fluxes (as inferred from interannual variations in
991 AGR) of temperature than precipitation, which is confirmed by our analysis of inversion-based
992 tropical land flux anomalies with climate variations (Fig 4). However, forest plot level
993 observations point to the prevailing drought as the dominant factor to reduce forest carbon
994 storage (Phillips et al., 2009). It remains challenging to reconcile the findings of temperature
995 dominance at large spatial scale and precipitation/moisture dominance at fine scale. Recently,
996 Jung et al. (2017) suggested that the dominant role of soil moisture over land carbon flux
997 anomalies has shifted to temperature when the scale of spatial aggregation increases, due to the
998 compensatory water effects in spatial upscaling. We also find that for all seasons except Q3,
999 inversion-based land carbon uptake anomalies in the tropics and southern extratropics are
1000 positively correlated with soil water content, with 2015 having an extreme low soil water content
1001 anomaly in Q4 (data not shown), echoing the extreme high temperature anomaly shown in Fig.
1002 S4I. This might indicate that temperature impacts the land carbon uptake mainly by increasing
1003 evaporative demand and decreasing soil water content. Besides, except Q1, we found no strong
1004 link between seasonal land carbon uptake anomalies and NDVI anomalies.

1005

1006 **4.3 Data uncertainties and perspective**

1007 On the global and hemispheric scales, the inversion-derived land- and ocean-atmosphere fluxes
1008 are well constrained by the observed atmospheric CO₂ growth rates on measurement sites.

1009 However, because the observational network is heterogeneous and sites are sparsely distributed
1010 (Supplementary Fig. S11), land CO₂ fluxes cannot be resolved precisely over each grid cell
1011 (Kaminski et al., 2001) and some regions are better constrained than others. This could hinder
1012 the precise pixel-scale matching between gridded CO₂ flux maps and climate states or the
1013 occurrence of climate extremes to investigate [how climate extreme impact carbon fluxes](#).
1014 [Although we have identified carbon uptake transitions for some regions and seasons might be](#)
1015 [related with certain climate extremes \(e.g., the role of precipitation in TeNH of Q4 shown in Fig.](#)
1016 [S5h\), but in general](#) exact attribution of carbon uptake transitions into different climate drivers
1017 could be elusive. Further, a few other uncertainties matter for the specific objective of this study.
1018 First, the atmospheric network increased over time, so that the inversions have a better ability to
1019 detect and quantify a sharp transition in CO₂ fluxes occurring in the last than in the first decade
1020 of the period analysed. This might hide the detection of other more extreme end-of-year carbon
1021 transitions during early years of our target period (1981-2015). Second, because measurements
1022 for the early 2016 are not used in the CAMS inversion and not completely available in the Jena
1023 inversion, the constraining of last season in 2015 is weaker than for the other three seasons. This
1024 could partly influence the exact magnitude of the extreme Q4 negative anomaly in land carbon
1025 uptake reported here. Third, the sparse sites located in the boreal Eurasia and tropical regions
1026 might diminish the ability of inversion systems to robustly allocation carbon fluxes spatially,
1027 which could yield high uncertainty in the carbon fluxes diagnosed for these regions (van der
1028 Laan-Luijkx et al., 2015; Stephens et al., 2007).

1029
1030 Despite these uncertainties, the strong transition of CO₂ fluxes from Q3 to Q4 analysed here is
1031 the largest ever found in the inversion records. [Although 2015 shows extreme greening in the](#)
1032 [northern hemisphere, this strong greenness has been only translated into a moderate annual](#)
1033 [carbon sink anomaly in 2015, because vegetation greenness and land uptake anomalies are](#)
1034 [largely decoupled outside growing season. The strong transition to carbon source in TeNH in Q4](#)
1035 [is consistent with extreme precipitation that might have largely increased respiration loss. In the](#)
1036 tropics, the transition to a strong source in TroSH in Q4 is congruent with the expected response
1037 of ecosystems to the peak of an El Niño event. [However, given the ambiguous findings regarding](#)
1038 [changes in vegetation greenness during dry seasons or drought periods by previous studies](#)
1039 [\(Saleska et al., 2007; Xu et al., 2011\), and the uncertain roles of climate variations in driving the](#)

1040 regional land carbon balance, more work is needed to reveal how these processes have evolved
1041 during opposing ENSO events. For the boreal and temperate Northern Hemisphere, further
1042 investigation is still needed to verify whether a coupling between strong spring/summer uptake
1043 and autumn release is something intrinsic to natural ecosystems, or if strong transitions to
1044 autumn release are triggered more by abrupt climate shifts. This could be evaluated by process-
1045 based and data-driven models to partition the overall sink anomaly into individual responses of
1046 photosynthesis and respiration, but that is beyond the scope of this work. Our results point to the
1047 need to better understand the drivers of carbon dynamics at seasonal, or even shorter time scales
1048 at the regional to global level, especially the link between such dynamics and climate extremes.
1049 Such understanding would help better predictions of the response of the carbon cycle to multiple
1050 long-term drivers such as atmospheric CO₂ growth and climate change.

1051

1052 **5 Conclusions**

1053 We investigated the links among vegetation greenness, interannual land carbon flux variations
1054 and climate variations for 1981–2015 using inversion-based land carbon flux data sets.
1055 Consistent positive correlations between satellite-derived vegetation greenness and land carbon
1056 uptakes are found for the northern hemisphere during growing season, but outside the growing
1057 season, vegetation greenness and land carbon uptake are largely decoupled. Carbon uptake in the
1058 boreal northern hemisphere (>45°N) is more consistently associated with temperature than
1059 precipitation, while such a pattern is less evident for the temperate northern hemisphere (23.5–
1060 45°N). Consistent with previous studies, we found a strong negative impact by temperature in
1061 the land carbon uptakes in tropics and southern hemisphere, probably driven by the role of
1062 temperature in soil water content.

1063

1064 We made an emphasis on the seasonal dynamics of land carbon uptake in 2015 due to its
1065 seeming paradox between the greatest vegetation greenness and the highest atmospheric CO₂
1066 growth rate. We found that lands in Northern Hemisphere started with a higher-than-normal sink
1067 for the northern growing seasons, consistent with enhanced vegetation greenness partly owing to
1068 elevated warming, however this enhanced sink was partly balanced by enhanced carbon release
1069 in autumn and winter, associated with extremely high precipitation in Q4 in temperate northern
1070 hemisphere (23.5–45°N). For tropics and Southern Hemisphere, a strong and abrupt transition

1071 toward a large carbon source for the last quarter of 2015 was found, concomitant with the peak
1072 of El Niño development. This strong transition of terrestrial CO₂ fluxes in the last quarter is the
1073 largest in the inversion records since 1981. The transitions in CO₂ fluxes diagnosed in this study
1074 form an interesting test bed for evaluating ecosystem models and gaining understanding of their
1075 controlling processes.

1076 **References**

- 1077 Adler, R. F., Huffman, G. J., Chang, A., Ferraro, R., Xie, P.-P., Janowiak, J., Rudolf, B.,
1078 Schneider, U., Curtis, S., Bolvin, D., Gruber, A., Susskind, J., Arkin, P. and Nelkin, E.: The
1079 Version-2 Global Precipitation Climatology Project (GPCP) Monthly Precipitation Analysis
1080 (1979–Present), *J. Hydrometeorol.*, 4(6), 1147–1167, doi:10.1175/1525-
1081 7541(2003)004<1147:TVGPCP>2.0.CO;2, 2003.
- 1082 Ahlström, A., Raupach, M. R., Schurgers, G., Smith, B., Arneeth, A., Jung, M., Reichstein, M.,
1083 Canadell, J. G., Friedlingstein, P., Jain, A. K., Kato, E., Poulter, B., Sitch, S., Stocker, B. D.,
1084 Viovy, N., Wang, Y. P., Wiltshire, A., Zaehle, S. and Zeng, N.: The dominant role of semi-
1085 arid ecosystems in the trend and variability of the land CO₂ sink, *Science*, 348(6237), 895–
1086 899, doi:10.1126/science.aaa1668, 2015.
- 1087 Angert, A., Biraud, S., Bonfils, C., Henning, C. C., Buermann, W., Pinzon, J., Tucker, C. J. and
1088 Fung, I.: Drier summers cancel out the CO₂ uptake enhancement induced by warmer springs,
1089 *Proc. Natl. Acad. Sci. U. S. A.*, 102(31), 10823–10827, doi:10.1073/pnas.0501647102, 2005.
- 1090 Ballantyne, A. P., Alden, C. B., Miller, J. B., Tans, P. P. and White, J. W. C.: Increase in
1091 observed net carbon dioxide uptake by land and oceans during the past 50 years, *Nature*,
1092 488(7409), 70–72, doi:10.1038/nature11299, 2012.
- 1093 Barichivich, J., Briffa, K. R., Myneni, R. B., Osborn, T. J., Melvin, T. M., Ciais, P., Piao, S. and
1094 Tucker, C.: Large-scale variations in the vegetation growing season and annual cycle of
1095 atmospheric CO₂ at high northern latitudes from 1950 to 2011, *Glob. Change Biol.*, 19(10),
1096 3167–3183, doi:10.1111/gcb.12283, 2013.
- 1097 Bastos, A., Ciais, P., Park, T., Zscheischler, J., Yue, C., Barichivich, J., Myneni, R. B., Peng, S.,
1098 Piao, S. and Zhu, Z.: Was the extreme Northern Hemisphere greening in 2015 predictable?,
1099 *Environ. Res. Lett.*, 12(4), 044016, doi:10.1088/1748-9326/aa67b5, 2017.
- 1100 Canadell, J. G., Le Quéré, C., Raupach, M. R., Field, C. B., Buitenhuis, E. T., Ciais, P., Conway,
1101 T. J., Gillett, N. P., Houghton, R. A. and Marland, G.: Contributions to accelerating
1102 atmospheric CO₂ growth from economic activity, carbon intensity, and efficiency of natural
1103 sinks, *Proc. Natl. Acad. Sci.*, 104(47), 18866–18870, 2007.
- 1104 Chen, J., Jönsson, P., Tamura, M., Gu, Z., Matsushita, B. and Eklundh, L.: A simple method for
1105 reconstructing a high-quality NDVI time-series data set based on the Savitzky–Golay filter,
1106 *Remote Sens. Environ.*, 91(3), 332–344, doi:10.1016/j.rse.2004.03.014, 2004.

1107 Chevallier, F., Fisher, M., Peylin, P., Serrar, S., Bousquet, P., Bréon, F.-M., Chédin, A. and
1108 Ciais, P.: Inferring CO₂ sources and sinks from satellite observations: Method and application
1109 to TOVS data, *J. Geophys. Res. Atmospheres*, 110(D24), D24309,
1110 doi:10.1029/2005JD006390, 2005.

1111 Chevallier, F., Ciais, P., Conway, T. J., Aalto, T., Anderson, B. E., Bousquet, P., Brunke, E. G.,
1112 Ciattaglia, L., Esaki, Y., Fröhlich, M., Gomez, A., Gomez-Pelaez, A. J., Haszpra, L.,
1113 Krummel, P. B., Langenfelds, R. L., Leuenberger, M., Machida, T., Maignan, F., Matsueda,
1114 H., Morguí, J. A., Mukai, H., Nakazawa, T., Peylin, P., Ramonet, M., Rivier, L., Sawa, Y.,
1115 Schmidt, M., Steele, L. P., Vay, S. A., Vermeulen, A. T., Wofsy, S. and Worthy, D.: CO₂
1116 surface fluxes at grid point scale estimated from a global 21 year reanalysis of atmospheric
1117 measurements, *J. Geophys. Res. Atmospheres*, 115(D21), D21307,
1118 doi:10.1029/2010JD013887, 2010.

1119 Cox, P. M., Pearson, D., Booth, B. B., Friedlingstein, P., Huntingford, C., Jones, C. D. and Luke,
1120 C. M.: Sensitivity of tropical carbon to climate change constrained by carbon dioxide
1121 variability, *Nature*, 494(7437), 341–344, doi:10.1038/nature11882, 2013.

1122 Dee, D. P., Uppala, S. M., Simmons, A. J., Berrisford, P., Poli, P., Kobayashi, S., Andrae, U.,
1123 Balmaseda, M. A., Balsamo, G., Bauer, P., Bechtold, P., Beljaars, A. C. M., van de Berg, L.,
1124 Bidlot, J., Bormann, N., Delsol, C., Dragani, R., Fuentes, M., Geer, A. J., Haimberger, L.,
1125 Healy, S. B., Hersbach, H., Hólm, E. V., Isaksen, I., Kållberg, P., Köhler, M., Matricardi, M.,
1126 McNally, A. P., Monge-Sanz, B. M., Morcrette, J.-J., Park, B.-K., Peubey, C., de Rosnay, P.,
1127 Tavolato, C., Thépaut, J.-N. and Vitart, F.: The ERA-Interim reanalysis: configuration and
1128 performance of the data assimilation system, *Q. J. R. Meteorol. Soc.*, 137(656), 553–597,
1129 doi:10.1002/qj.828, 2011.

1130 Didan K 2015 MOD13C1 MODIS/Terra Vegetation Indices 16-Day L3 Global 0.05Deg CMG
1131 V006 NASA EOSDIS Land Processes DAAC ([https://doi.org/10.5067/MODIS/](https://doi.org/10.5067/MODIS/MOD13C1.006)
1132 [MOD13C1.006](https://doi.org/10.5067/MODIS/MOD13C1.006))

1133 Doughty, C. E., Metcalfe, D. B., Girardin, C. a. J., Amézquita, F. F., Cabrera, D. G., Huasco, W.
1134 H., Silva-Espejo, J. E., Araujo-Murakami, A., da Costa, M. C., Rocha, W., Feldpausch, T. R.,
1135 Mendoza, A. L. M., da Costa, A. C. L., Meir, P., Phillips, O. L. and Malhi, Y.: Drought
1136 impact on forest carbon dynamics and fluxes in Amazonia, *Nature*, 519(7541), 78–82,
1137 doi:10.1038/nature14213, 2015.

1138 Forkel, M., Carvalhais, N., Rödenbeck, C., Keeling, R., Heimann, M., Thonicke, K., Zaehle, S.
1139 and Reichstein, M.: Enhanced seasonal CO₂ exchange caused by amplified plant productivity
1140 in northern ecosystems, *Science*, 351(6274), 696–699, doi:10.1126/science.aac4971, 2016.

1141 Gamon, J. A., Field, C. B., Goulden, M. L., Griffin, K. L., Hartley, A. E., Joel, G., Peñuelas, J.
1142 and Valentini, R.: Relationships Between NDVI, Canopy Structure, and Photosynthesis in
1143 Three Californian Vegetation Types, *Ecol. Appl.*, 5(1), 28–41, doi:10.2307/1942049, 1995.

1144 Graven, H. D., Keeling, R. F., Piper, S. C., Patra, P. K., Stephens, B. B., Wofsy, S. C., Welp, L.
1145 R., Sweeney, C., Tans, P. P., Kelley, J. J., Daube, B. C., Kort, E. A., Santoni, G. W. and Bent,
1146 J. D.: Enhanced Seasonal Exchange of CO₂ by Northern Ecosystems Since 1960, *Science*,
1147 341(6150), 1085–1089, doi:10.1126/science.1239207, 2013.

1148 Gu, L., Baldocchi, D. D., Wofsy, S. C., Munger, J. W., Michalsky, J. J., Urbanski, S. P. and
1149 Boden, T. A.: Response of a Deciduous Forest to the Mount Pinatubo Eruption: Enhanced
1150 Photosynthesis, *Science*, 299(5615), 2035–2038, doi:10.1126/science.1078366, 2003.

1151 Hadden, D. and Grelle, A.: Changing temperature response of respiration turns boreal forest
1152 from carbon sink into carbon source, *Agric. For. Meteorol.*, 223, 30–38,
1153 doi:10.1016/j.agrformet.2016.03.020, 2016.

1154 Huete, A. R., Didan, K., Shimabukuro, Y. E., Ratana, P., Saleska, S. R., Hutrya, L. R., Yang, W.,
1155 Nemani, R. R. and Myneni, R.: Amazon rainforests green-up with sunlight in dry season,
1156 *Geophys. Res. Lett.*, 33(6), L06405, doi:10.1029/2005GL025583, 2006.

1157 Huijnen, V., Wooster, M. J., Kaiser, J. W., Gaveau, D. L. A., Flemming, J., Parrington, M.,
1158 Inness, A., Murdiyarso, D., Main, B. and Weele, M. van: Fire carbon emissions over maritime
1159 southeast Asia in 2015 largest since 1997, *Sci. Rep.*, 6, 26886, doi:10.1038/srep26886, 2016.

1160 Jacobson, A. R., Mikaloff Fletcher, S. E., Gruber, N., Sarmiento, J. L. and Gloor, M.: A joint
1161 atmosphere-ocean inversion for surface fluxes of carbon dioxide: 1. Methods and global-scale
1162 fluxes, *Glob. Biogeochem. Cycles*, 21(1), GB1019, doi:10.1029/2005GB002556, 2007.

1163 Jiménez-Muñoz, J. C., Mattar, C., Barichivich, J., Santamaría-Artigas, A., Takahashi, K., Malhi,
1164 Y., Sobrino, J. A. and Schrier, G. van der: Record-breaking warming and extreme drought in
1165 the Amazon rainforest during the course of El Niño 2015–2016, *Sci. Rep.*, 6, 33130,
1166 doi:10.1038/srep33130, 2016.

1167 Jönsson, P. and Eklundh, L.: TIMESAT—a program for analyzing time-series of satellite sensor
1168 data, *Comput. Geosci.*, 30(8), 833–845, doi:10.1016/j.cageo.2004.05.006, 2004.

1169 Jung, M., Reichstein, M., Schwalm, C. R., Huntingford, C., Sitch, S., Ahlström, A., Arneth, A.,
1170 Camps-Valls, G., Ciais, P., Friedlingstein, P. and others: Compensatory water effects link
1171 yearly global land CO₂ sink changes to temperature, *Nature* [online] Available from:
1172 <https://www.nature.com/nature/journal/vaop/ncurrent/full/nature20780.html> (Accessed 19
1173 June 2017), 2017.

1174 Kaminski, T., Rayner, P. J., Heimann, M. and Enting, I. G.: On aggregation errors in
1175 atmospheric transport inversions, *J. Geophys. Res. Atmospheres*, 106(D5), 4703–4715,
1176 doi:10.1029/2000JD900581, 2001.

1177 van der Laan-Luijkx, I. T., van der Velde, I. R., Krol, M. C., Gatti, L. V., Domingues, L. G.,
1178 Correia, C. S. C., Miller, J. B., Gloor, M., van Leeuwen, T. T., Kaiser, J. W., Wiedinmyer, C.,
1179 Basu, S., Clerbaux, C. and Peters, W.: Response of the Amazon carbon balance to the 2010
1180 drought derived with CarbonTracker South America, *Glob. Biogeochem. Cycles*, 29(7),
1181 2014GB005082, doi:10.1002/2014GB005082, 2015.

1182 Lewis, S. L., Brando, P. M., Phillips, O. L., van der Heijden, G. M. and Nepstad, D.: The 2010
1183 amazon drought, *Science*, 331(6017), 554–554, 2011.

1184 Li, W., Ciais, P., Wang, Y., Peng, S., Broquet, G., Ballantyne, A. P., Canadell, J. G., Cooper, L.,
1185 Friedlingstein, P., Quéré, C. L., Myneni, R. B., Peters, G. P., Piao, S. and Pongratz, J.:
1186 Reducing uncertainties in decadal variability of the global carbon budget with multiple
1187 datasets, *Proc. Natl. Acad. Sci.*, 113(46), 13104–13108, doi:10.1073/pnas.1603956113, 2016.

1188 Medlyn, B. E.: Comment on “Drought-Induced Reduction in Global Terrestrial Net Primary
1189 Production from 2000 Through 2009,” *Science*, 333(6046), 1093–1093,
1190 doi:10.1126/science.1199544, 2011.

1191 Morton, D. C., Nagol, J., Carabajal, C. C., Rosette, J., Palace, M., Cook, B. D., Vermote, E. F.,
1192 Harding, D. J. and North, P. R. J.: Amazon forests maintain consistent canopy structure and
1193 greenness during the dry season, *Nature*, 506(7487), 221–224, doi:10.1038/nature13006,
1194 2014.

1195 Myneni, R. B., Keeling, C. D., Tucker, C. J., Asrar, G. and Nemani, R. R.: Increased plant
1196 growth in the northern high latitudes from 1981 to 1991, *Nature*, 386(6626), 698–702,
1197 doi:10.1038/386698a0, 1997.

1198 Nemani, R. R., Keeling, C. D., Hashimoto, H., Jolly, W. M., Piper, S. C., Tucker, C. J., Myneni,
1199 R. B. and Running, S. W.: Climate-Driven Increases in Global Terrestrial Net Primary

1200 Production from 1982 to 1999, *Science*, 300(5625), 1560–1563,
1201 doi:10.1126/science.1082750, 2003.

1202 Orth, R., Zscheischler, J. and Seneviratne, S. I.: Record dry summer in 2015 challenges
1203 precipitation projections in Central Europe, *Sci. Rep.*, 6, 28334, doi:10.1038/srep28334, 2016.

1204 Phillips, O. L., Aragão, L. E. O. C., Lewis, S. L., Fisher, J. B., Lloyd, J., López-González, G.,
1205 Malhi, Y., Monteagudo, A., Peacock, J., Quesada, C. A., Heijden, G. van der, Almeida, S.,
1206 Amaral, I., Arroyo, L., Aymard, G., Baker, T. R., Bánki, O., Blanc, L., Bonal, D., Brando, P.,
1207 Chave, J., Oliveira, Á. C. A. de, Cardozo, N. D., Czimczik, C. I., Feldpausch, T. R., Freitas,
1208 M. A., Gloor, E., Higuchi, N., Jiménez, E., Lloyd, G., Meir, P., Mendoza, C., Morel, A., Neill,
1209 D. A., Nepstad, D., Patiño, S., Peñuela, M. C., Prieto, A., Ramírez, F., Schwarz, M., Silva, J.,
1210 Silveira, M., Thomas, A. S., Steege, H. ter, Stropp, J., Vásquez, R., Zelazowski, P., Dávila, E.
1211 A., Andelman, S., Andrade, A., Chao, K.-J., Erwin, T., Fiore, A. D., C, E. H., Keeling, H.,
1212 Killeen, T. J., Laurance, W. F., Cruz, A. P., Pitman, N. C. A., Vargas, P. N., Ramírez-Angulo,
1213 H., Rudas, A., Salamão, R., Silva, N., Terborgh, J. and Torres-Lezama, A.: Drought
1214 Sensitivity of the Amazon Rainforest, *Science*, 323(5919), 1344–1347,
1215 doi:10.1126/science.1164033, 2009.

1216 Piao, S., Ciais, P., Friedlingstein, P., Peylin, P., Reichstein, M., Luysaert, S., Margolis, H.,
1217 Fang, J., Barr, A., Chen, A., Grelle, A., Hollinger, D. Y., Laurila, T., Lindroth, A.,
1218 Richardson, A. D. and Vesala, T.: Net carbon dioxide losses of northern ecosystems in
1219 response to autumn warming, *Nature*, 451(7174), 49–52, doi:10.1038/nature06444, 2008.

1220 Piao, S., Nan, H., Huntingford, C., Ciais, P., Friedlingstein, P., Sitch, S., Peng, S., Ahlström, A.,
1221 Canadell, J. G., Cong, N., Levis, S., Levy, P. E., Liu, L., Lomas, M. R., Mao, J., Myneni, R.
1222 B., Peylin, P., Poulter, B., Shi, X., Yin, G., Viovy, N., Wang, T., Wang, X., Zaehle, S., Zeng,
1223 N., Zeng, Z. and Chen, A.: Evidence for a weakening relationship between interannual
1224 temperature variability and northern vegetation activity, *Nat. Commun.*, 5, 5018,
1225 doi:10.1038/ncomms6018, 2014.

1226 Poulter, B., Frank, D., Ciais, P., Myneni, R. B., Andela, N., Bi, J., Broquet, G., Canadell, J. G.,
1227 Chevallier, F., Liu, Y. Y., Running, S. W., Sitch, S. and van der Werf, G. R.: Contribution of
1228 semi-arid ecosystems to interannual variability of the global carbon cycle, *Nature*, 509(7502),
1229 600–603, doi:10.1038/nature13376, 2014.

1230 Prather, M. J., Holmes, C. D. and Hsu, J.: Reactive greenhouse gas scenarios: Systematic

1231 exploration of uncertainties and the role of atmospheric chemistry, *Geophys. Res. Lett.*, 39(9),
1232 L09803, doi:10.1029/2012GL051440, 2012.

1233 Quéré, C. L., Andrew, R. M., Canadell, J. G., Sitch, S., Korsbakken, J. I., Peters, G. P., Manning,
1234 A. C., Boden, T. A., Tans, P. P., Houghton, R. A., Keeling, R. F., Alin, S., Andrews, O. D.,
1235 Anthoni, P., Barbero, L., Bopp, L., Chevallier, F., Chini, L. P., Ciais, P., Currie, K., Delire,
1236 C., Doney, S. C., Friedlingstein, P., Gkritzalis, T., Harris, I., Hauck, J., Haverd, V., Hoppema,
1237 M., Klein Goldewijk, K., Jain, A. K., Kato, E., Körtzinger, A., Landschützer, P., Lefèvre, N.,
1238 Lenton, A., Lienert, S., Lombardozzi, D., Melton, J. R., Metzl, N., Millero, F., Monteiro, P.
1239 M. S., Munro, D. R., Nabel, J. E. M. S., Nakaoka, S., O'Brien, K., Olsen, A., Omar, A. M.,
1240 Ono, T., Pierrot, D., Poulter, B., Rödenbeck, C., Salisbury, J., Schuster, U., Schwinger, J.,
1241 Séférian, R., Skjelvan, I., Stocker, B. D., Sutton, A. J., Takahashi, T., Tian, H., Tilbrook, B.,
1242 Laan-Luijckx, I. T. van der, Werf, G. R. van der, Viovy, N., Walker, A. P., Wiltshire, A. J. and
1243 Zaehle, S.: Global Carbon Budget 2016, *Earth Syst. Sci. Data*, 8(2), 605–649,
1244 doi:10.5194/essd-8-605-2016, 2016.

1245 Rödenbeck, C.: Estimating CO₂ sources and sinks from atmospheric mixing ratio measurements
1246 using a global inversion of atmospheric transport, Max Planck Institute for Biogeochemistry.,
1247 2005.

1248 Rödenbeck, C., Houweling, S., Gloor, M. and Heimann, M.: CO₂ flux history 1982–2001
1249 inferred from atmospheric data using a global inversion of atmospheric transport, *Atmos*
1250 *Chem Phys*, 3(6), 1919–1964, doi:10.5194/acp-3-1919-2003, 2003.

1251 Saleska, S. R., Didan, K., Huete, A. R. and Rocha, H. R. da: Amazon Forests Green-Up During
1252 2005 Drought, *Science*, 318(5850), 612–612, doi:10.1126/science.1146663, 2007.

1253 Samanta, A., Ganguly, S., Hashimoto, H., Devadiga, S., Vermote, E., Knyazikhin, Y., Nemani,
1254 R. R. and Myneni, R. B.: Amazon forests did not green-up during the 2005 drought, *Geophys.*
1255 *Res. Lett.*, 37(5), L05401, doi:10.1029/2009GL042154, 2010.

1256 Samanta, A., Costa, M. H., Nunes, E. L., Vieira, S. A., Xu, L. and Myneni, R. B.: Comment on
1257 “Drought-Induced Reduction in Global Terrestrial Net Primary Production from 2000
1258 Through 2009,” *Science*, 333(6046), 1093–1093, doi:10.1126/science.1199048, 2011.

1259 Stephens, B. B., Gurney, K. R., Tans, P. P., Sweeney, C., Peters, W., Bruhwiler, L., Ciais, P.,
1260 Ramonet, M., Bousquet, P., Nakazawa, T., Aoki, S., Machida, T., Inoue, G., Vinnichenko, N.,
1261 Lloyd, J., Jordan, A., Heimann, M., Shibistova, O., Langenfelds, R. L., Steele, L. P., Francey,

1262 R. J. and Denning, A. S.: Weak Northern and Strong Tropical Land Carbon Uptake from
1263 Vertical Profiles of Atmospheric CO₂, *Science*, 316(5832), 1732–1735,
1264 doi:10.1126/science.1137004, 2007.

1265 Tanja, S., Berninger, F., Vesala, T., Markkanen, T., Hari, P., Mäkelä, A., Ilvesniemi, H.,
1266 Hänninen, H., Nikinmaa, E., Huttula, T., Laurila, T., Aurela, M., Grelle, A., Lindroth, A.,
1267 Arneth, A., Shibistova, O. and Lloyd, J.: Air temperature triggers the recovery of evergreen
1268 boreal forest photosynthesis in spring, *Glob. Change Biol.*, 9(10), 1410–1426,
1269 doi:10.1046/j.1365-2486.2003.00597.x, 2003.

1270 Ueyama, M., Iwata, H. and Harazono, Y.: Autumn warming reduces the CO₂ sink of a black
1271 spruce forest in interior Alaska based on a nine-year eddy covariance measurement, *Glob.*
1272 *Change Biol.*, 20(4), 1161–1173, doi:10.1111/gcb.12434, 2014.

1273 Wang, W., Ciais, P., Nemani, R. R., Canadell, J. G., Piao, S., Sitch, S., White, M. A., Hashimoto,
1274 H., Milesi, C. and Myneni, R. B.: Variations in atmospheric CO₂ growth rates coupled with
1275 tropical temperature, *Proc. Natl. Acad. Sci.*, 110(32), 13061–13066,
1276 doi:10.1073/pnas.1219683110, 2013.

1277 Wang, X., Piao, S., Ciais, P., Friedlingstein, P., Myneni, R. B., Cox, P., Heimann, M., Miller, J.,
1278 Peng, S., Wang, T., Yang, H. and Chen, A.: A two-fold increase of carbon cycle sensitivity to
1279 tropical temperature variations, *Nature*, 506(7487), 212–215, doi:10.1038/nature12915, 2014.

1280 van der Werf, G. R., Randerson, J. T., Collatz, G. J., Giglio, L., Kasibhatla, P. S., Arellano, A.
1281 F., Olsen, S. C. and Kasischke, E. S.: Continental-Scale Partitioning of Fire Emissions During
1282 the 1997 to 2001 El Niño/La Niña Period, *Science*, 303(5654), 73–76,
1283 doi:10.1126/science.1090753, 2004.

1284 van der Werf, G. R., Dempewolf, J., Trigg, S. N., Randerson, J. T., Kasibhatla, P. S., Giglio, L.,
1285 Murdiyarso, D., Peters, W., Morton, D. C., Collatz, G. J., Dolman, A. J. and DeFries, R. S.:
1286 Climate regulation of fire emissions and deforestation in equatorial Asia, *Proc. Natl. Acad.*
1287 *Sci. U. S. A.*, 105(51), 20350–20355, doi:10.1073/pnas.0803375105, 2008.

1288 Wolf, S., Keenan, T. F., Fisher, J. B., Baldocchi, D. D., Desai, A. R., Richardson, A. D., Scott,
1289 R. L., Law, B. E., Litvak, M. E., Brunsell, N. A., Peters, W. and Laan-Luijkx, I. T. van der:
1290 Warm spring reduced carbon cycle impact of the 2012 US summer drought, *Proc. Natl. Acad.*
1291 *Sci.*, 113(21), 5880–5885, doi:10.1073/pnas.1519620113, 2016.

1292 Wolter, K. and Timlin, M. S.: El Niño/Southern Oscillation behaviour since 1871 as diagnosed

1293 in an extended multivariate ENSO index (MEI.ext), *Int. J. Climatol.*, 31(7), 1074–1087,
1294 doi:10.1002/joc.2336, 2011.

1295 Wu, J., Albert, L. P., Lopes, A. P., Restrepo-Coupe, N., Hayek, M., Wiedemann, K. T., Guan,
1296 K., Stark, S. C., Christoffersen, B., Prohaska, N., Tavares, J. V., Marostica, S., Kobayashi, H.,
1297 Ferreira, M. L., Campos, K. S., Silva, R. da, Brando, P. M., Dye, D. G., Huxman, T. E.,
1298 Huete, A. R., Nelson, B. W. and Saleska, S. R.: Leaf development and demography explain
1299 photosynthetic seasonality in Amazon evergreen forests, *Science*, 351(6276), 972–976,
1300 doi:10.1126/science.aad5068, 2016.

1301 Xu, L., Samanta, A., Costa, M. H., Ganguly, S., Nemani, R. R. and Myneni, R. B.: Widespread
1302 decline in greenness of Amazonian vegetation due to the 2010 drought, *Geophys. Res. Lett.*,
1303 38(7), L07402, doi:10.1029/2011GL046824, 2011.

1304 Yin, Y., Ciais, P., Chevallier, F., van der Werf, G. R., Fanin, T., Broquet, G., Boesch, H., Cozic,
1305 A., Hauglustaine, D., Szopa, S. and Wang, Y.: Variability of fire carbon emissions in
1306 equatorial Asia and its nonlinear sensitivity to El Niño, *Geophys. Res. Lett.*, 2016GL070971,
1307 doi:10.1002/2016GL070971, 2016.

1308 Zhao, M. and Running, S. W.: Drought-Induced Reduction in Global Terrestrial Net Primary
1309 Production from 2000 Through 2009, *Science*, 329(5994), 940–943,
1310 doi:10.1126/science.1192666, 2010.

1311 Zhou, L., Tucker, C. J., Kaufmann, R. K., Slayback, D., Shabanov, N. V. and Myneni, R. B.:
1312 Variations in northern vegetation activity inferred from satellite data of vegetation index
1313 during 1981 to 1999, *J. Geophys. Res. Atmospheres*, 106(D17), 20069–20083,
1314 doi:10.1029/2000JD000115, 2001.

1315

1316 **Acknowledgements**

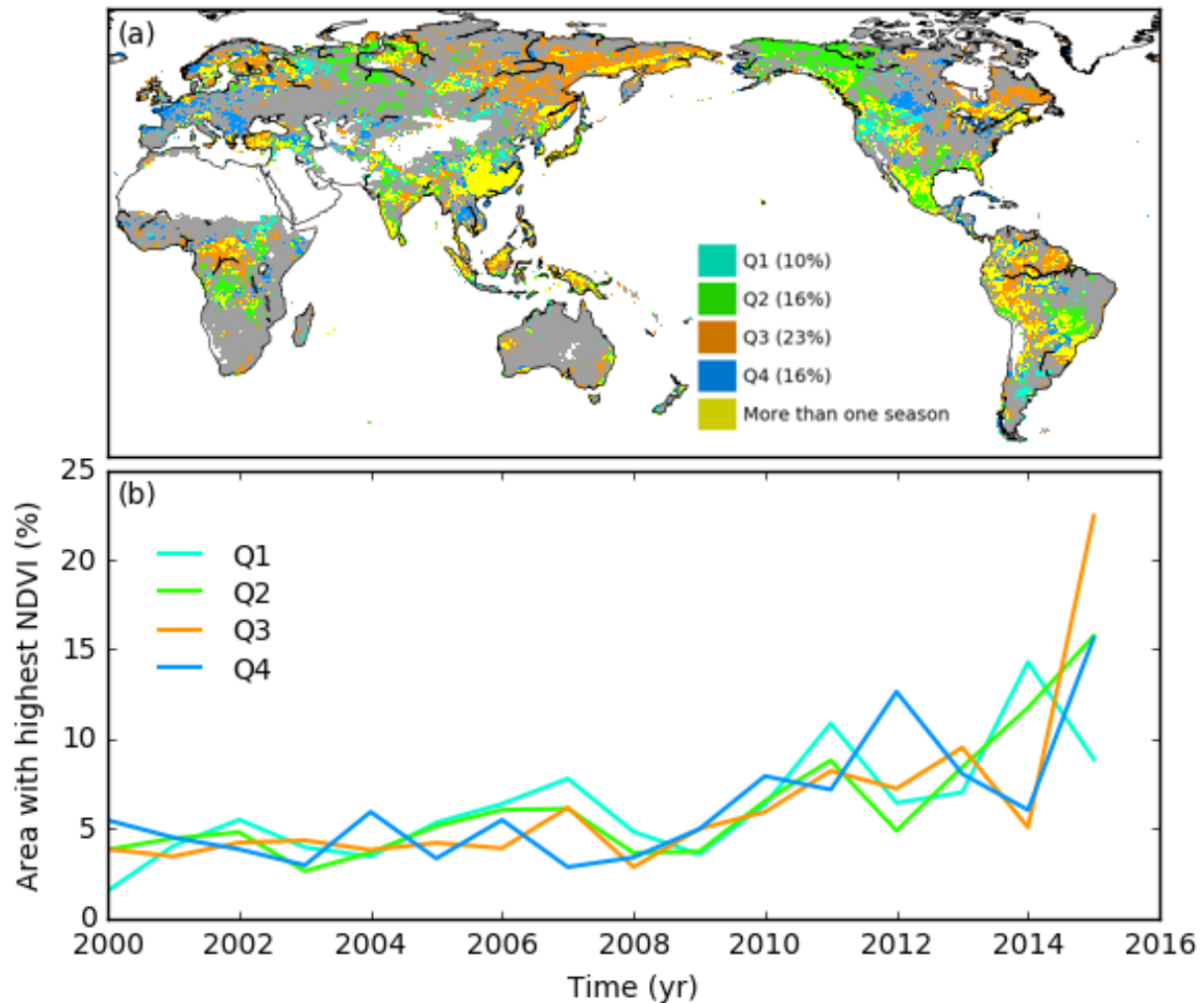
1317 C.Y. and P.C. acknowledge funding from the European Commission's 7th Framework
1318 Programme, under grant agreement number 603542 (LUC4C). The work of F.C. was funded by
1319 the Copernicus Atmosphere Monitoring Service, implemented by the European Centre for
1320 Medium-Range Weather Forecasts (ECMWF) on behalf of the European Commission. Taejin
1321 Park was supported by the NASA Earth and Space Science Fellowship Program (grant no.
1322 NNX16AO34H). We thank all the scientists involved in the surface and aircraft measurement of
1323 atmospheric CO₂ concentration and in archiving these data and making them available. We also

1324 thank Dr. Matthias Forkel and the anonymous reviewer for their review comments that helped
1325 improving the manuscript quality.

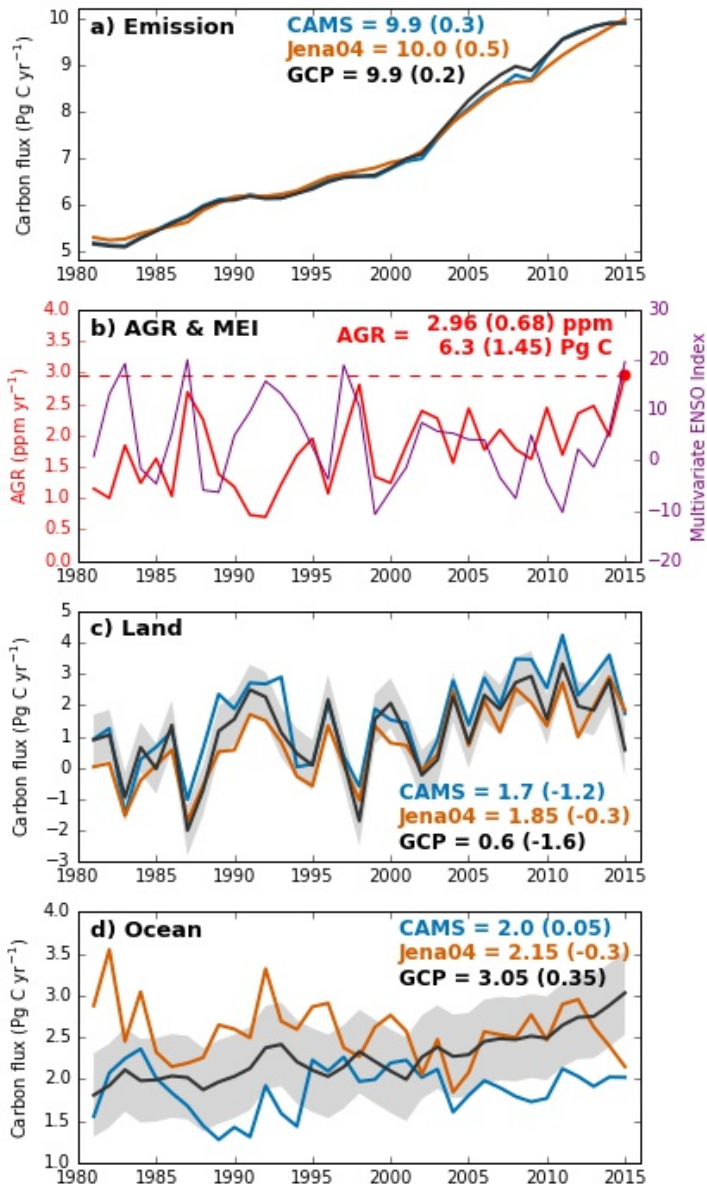
1326

1327 **Author contributions**

1328 P.C., F.C., C.Y. and A.B. conceived the study. C.Y. performed the analysis and made the first
1329 draft. F.C. and C.R. provided the inversion data. T. P. provided the NDVI data. All authors
1330 contributed to the interpretation of the results and writing of the paper.



1331
 1332 **Figure 1** Year 2015 as the greenest year over the period 2000-2015. (a) Distribution of seasons
 1333 for which 2015 NDVI ranks the highest during the period 2000-2015. Yellow-coloured pixels
 1334 indicate grid cells where 2015 NDVI ranks highest for more than one season. For each season,
 1335 the fraction of global vegetated land area for which 2015 NDVI ranks highest is shown in the
 1336 inset colour bar. (b) Temporal evolution of the percentage of vegetated land with highest NDVI
 1337 over 2000-2015 for each season and different years. The sum total of vertical-axis values for
 1338 each season over all years is 100%. Q1 = January–March; Q2 = April–June; Q3 = July–
 1339 September; Q4 = October–December.



1340

1341 **Figure 2** Global carbon fluxes and atmospheric CO₂ growth rates for 1981–2015. (a) Carbon
1342 emissions from fossil fuel and industry used in the CAMS (blue) and Jena04 (orange) inversions,

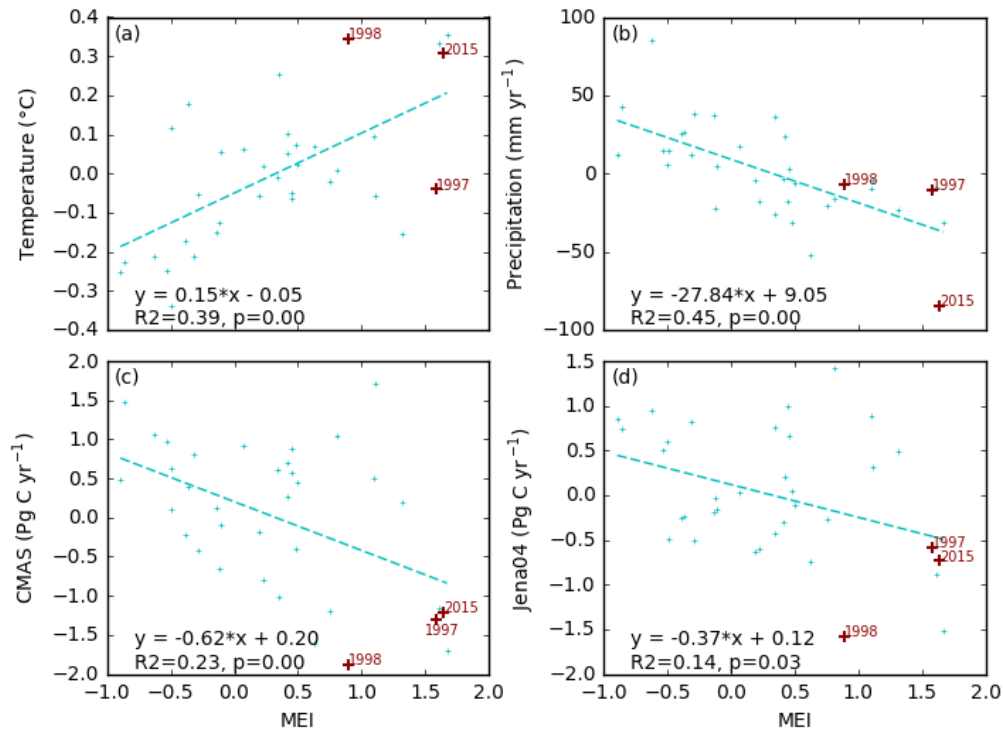
1343 (b) annual atmospheric CO₂ growth rate (AGR, in red) from NOAA/ESRL linked with
1344 Multivariate ENSO Index (in purple), and (c) land and (d) ocean carbon sinks for 1981-2015.

1345 Emissions and land and ocean carbon sinks from the Global Carbon Project (GCP, in black) are
1346 also shown for comparison. In subplots c and d, a carbon flux of 0.45 Pg C yr⁻¹ was used to

1347 correct inversion-derived land and ocean sinks to account for pre-industrial land-to-ocean carbon
1348 flux as in Le Quéré et al. (2016). All numbers indicate values in 2015 (Pg C yr⁻¹, rounded to

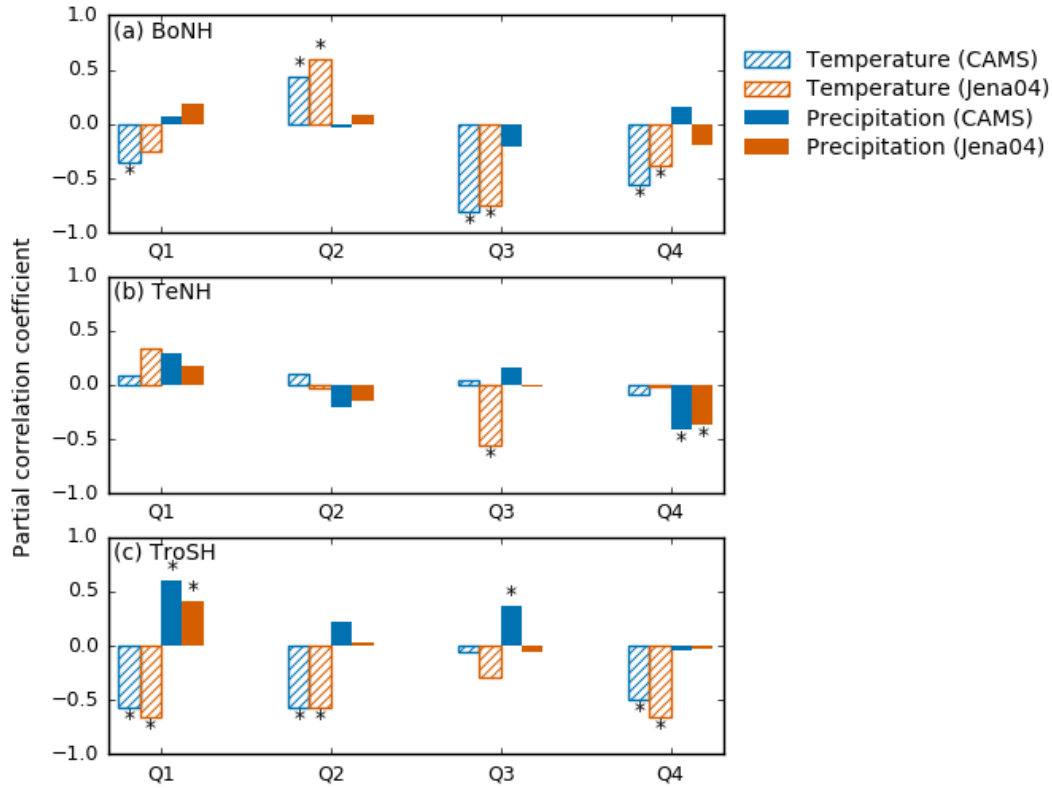
1349 ±0.05 Pg C yr⁻¹), with those in brackets showing linearly de-trended anomalies for the same

1350 year.
1351



1352
1353 **Figure 3** Relationships between anomalies of (a) land air temperature, (b) land precipitation, (c)
1354 land carbon fluxes by the CAMS inversion, (d) land carbon fluxes by the Jena04 inversion, and
1355 the Multivariate ENSO Index (MEI). All variables are linearly de-trended over 1981–2015.
1356

1357



1358

1359

1360 **Figure 4** Partial correlation coefficients of de-trended annual anomalies of land carbon fluxes by
1361 CAMS and Jena04 inversions against the anomalies in temperature and precipitation of different
1362 seasons. $n = 34$. The asterisk indicates significant correlation ($p < 0.05$).

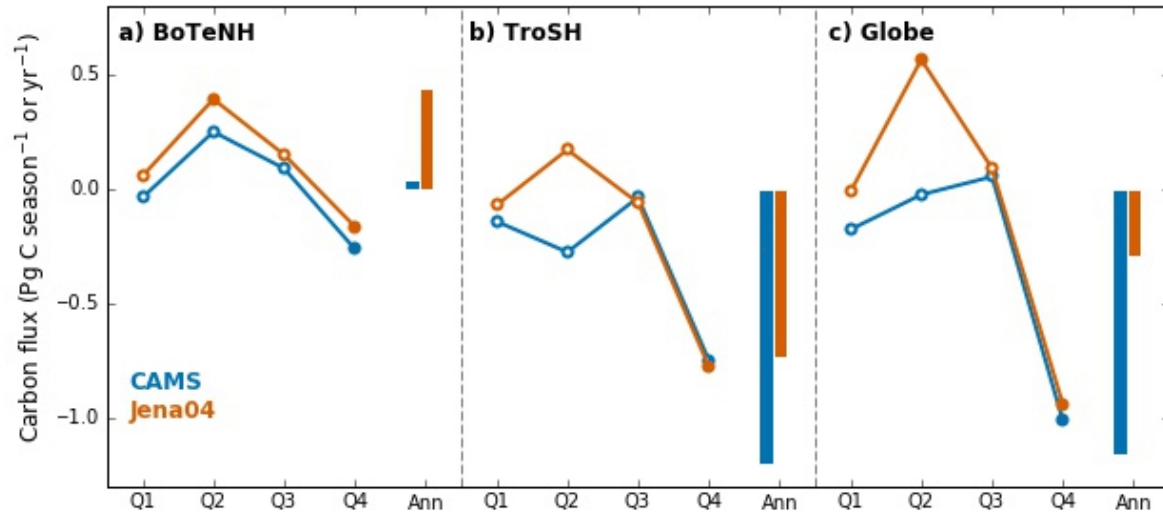


Figure 5 Seasonal land carbon uptake anomalies in 2015. Data are linearly de-trended over 1981-2015 for different seasons in 2015, by CAMS (blue) and Jena04 (orange) inversion data. Open or solid dots indicate seasonal values (Pg C season^{-1}) and vertical bars indicate annual sum (Pg C yr^{-1}). Data are shown for: (a) boreal and temperate Northern Hemisphere (BoTeNH, $> 23.5^\circ\text{N}$), (b) tropics and southern extratropical hemisphere (TroSH, $< 23.5^\circ\text{N}$) and (c) the whole globe. Solid dots indicate seasonal land carbon uptake anomalies below 10th or above 90th percentiles over 1981-2015.

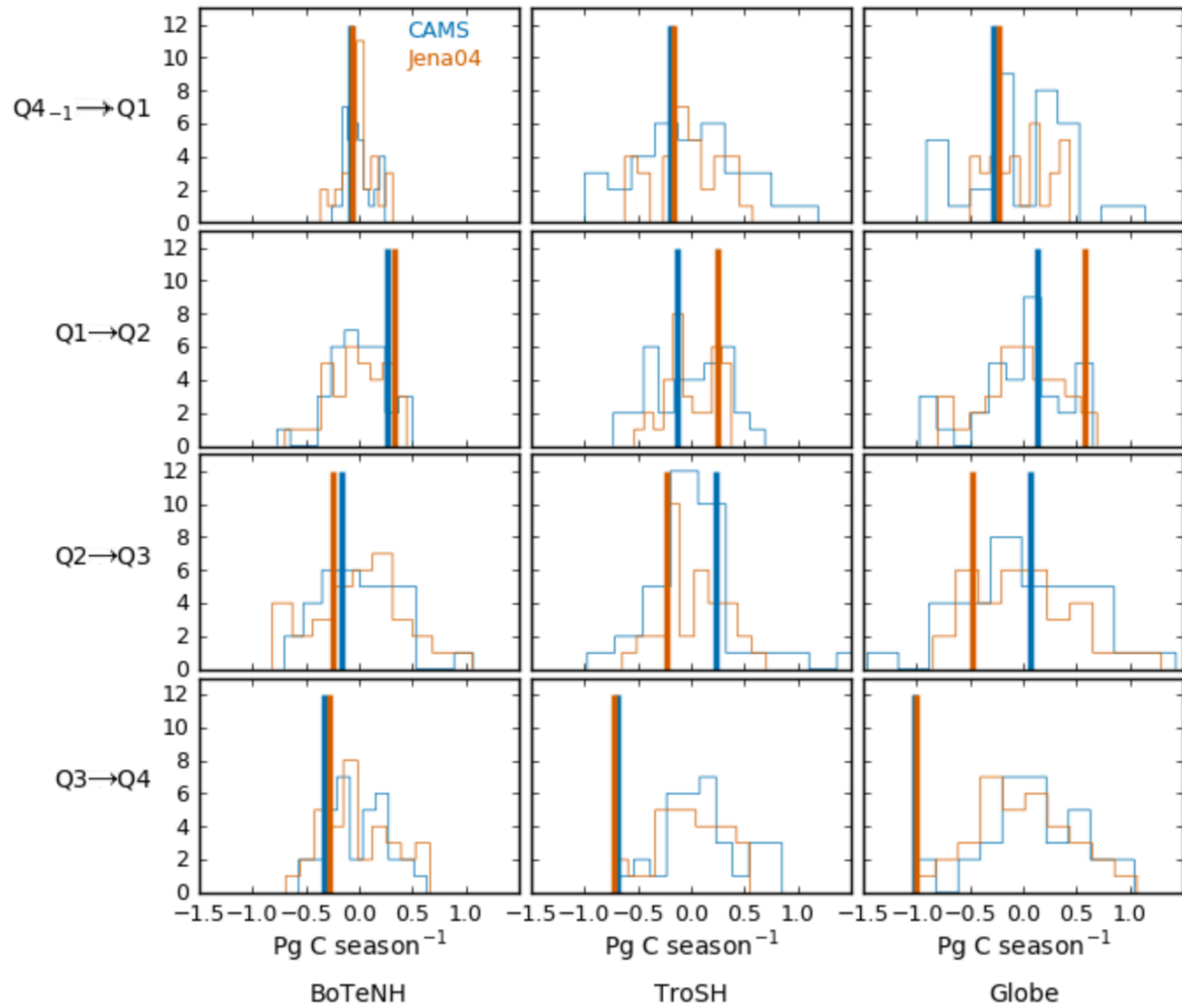


Figure 6 Extremeness of transitions in seasonal land carbon uptake anomaly in 2015. Lines of histograms for seasonal land carbon uptake transitions over 1981-2015 are shown for boreal and temperate Northern Hemisphere (BoTeNH, latitude $> 23.5^{\circ}\text{N}$), tropics and extratropical Southern Hemisphere (TroSH, latitude $< 23.5^{\circ}\text{N}$) and the whole globe. Transition between two consecutive seasons is defined as the linearly de-trended land carbon uptake anomaly in a given season minus that in the former one. X-axis shows the seasonal transitions in land carbon uptake anomalies (Pg C season^{-1}). Vertical orange solid lines indicate values for 2015.